Supporting information

for

[Re(CO)₃]⁺ complexes of exo-functionalized tridentate "click" macrocycles: Synthesis, stability, photophysical properties, bio-conjugation and antibacterial activity

Asif Noor,[a] Gregory S. Huff,[a,b] Sreedhar V. Kumar,[a,c] James E. M. Lewis,[a] Brett M. Paterson,[d] Christine Schieber,[d] Paul S. Donnelly,[d] Heather J. L. Brooks,[c] Keith C. Gordon,[a,b] Stephen C. Moratti,[a,b] and James D. Crowley,[a,]*

[a]Department of Chemistry, University of Otago, PO Box 56, Dunedin, New Zealand.

[b]MacDiarmid Institute for Advanced Materials and Nanotechnology, New Zealand.

[c]Department of Microbiology and Immunology, Otago School of Medical Sciences, University of Otago, Dunedin, New Zealand.

[d]School of Chemistry and Bio21 Molecular Science Biotechnology Institute, University of Melbourne, Melbourne 3010, Australia.

E-mail: jcrowley@chemistry.otago.ac.nz

Fax: +64 3 479 7906; Tel: +64 3 479 7731.

KEYWORDS: macrocycles, CuAAC, click, Re(I), 1,2,3-triazole, pyridyl.

Contents

1 Selected ^{1}H NMR and HR-ESI-MS spectra of synthesized compounds

Macrocycle, 7
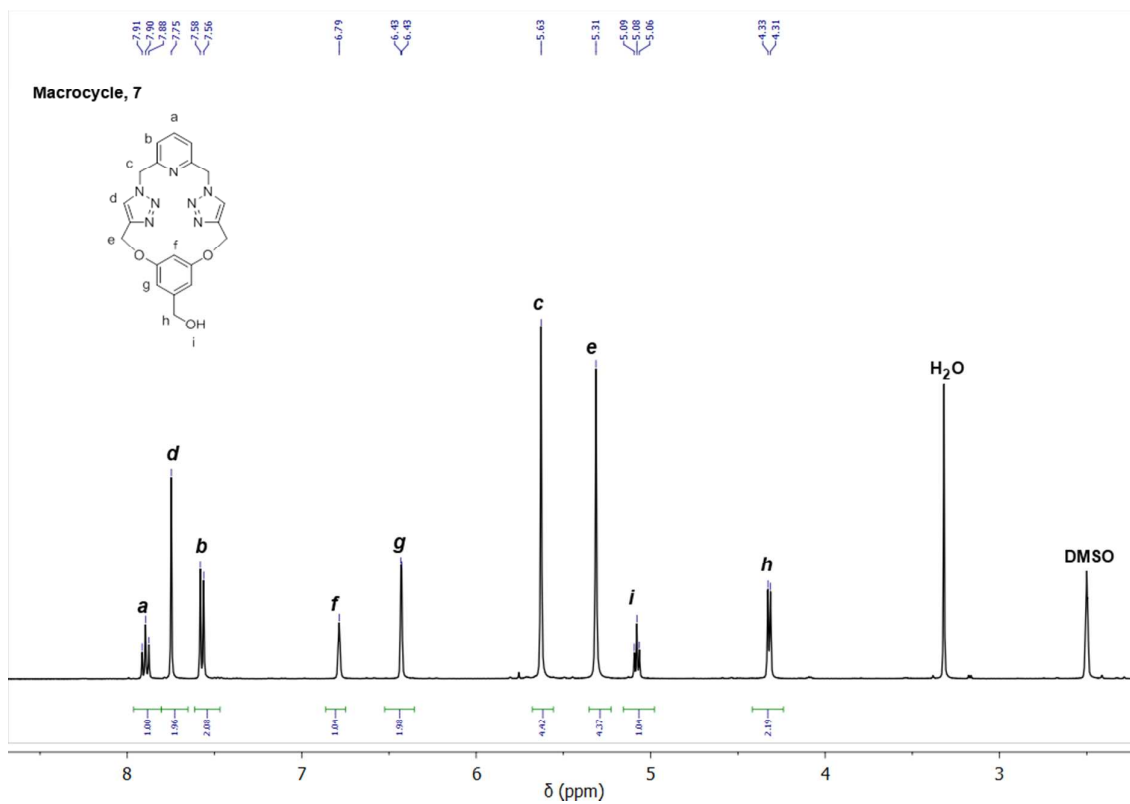
Figure S 1 ^{1}H NMR spectrum (400 MHz, DMSO-d_6, 298 K) of macrocycle **7**
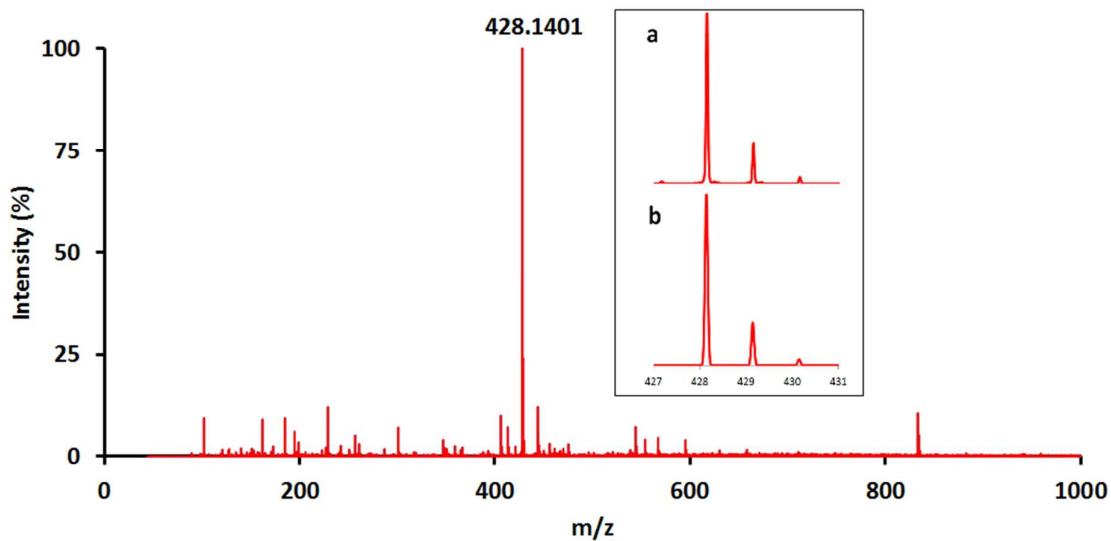

Figure S 2 HR-ESI-MS spectrum of macrocycle **7**, inset a) observed and b) calculated isotopic patterns for the peaks at m/z = 428.1404 due to $[\mathbf{7}+\text{Na}]^{+}$ ion.

Macrocycle, 8
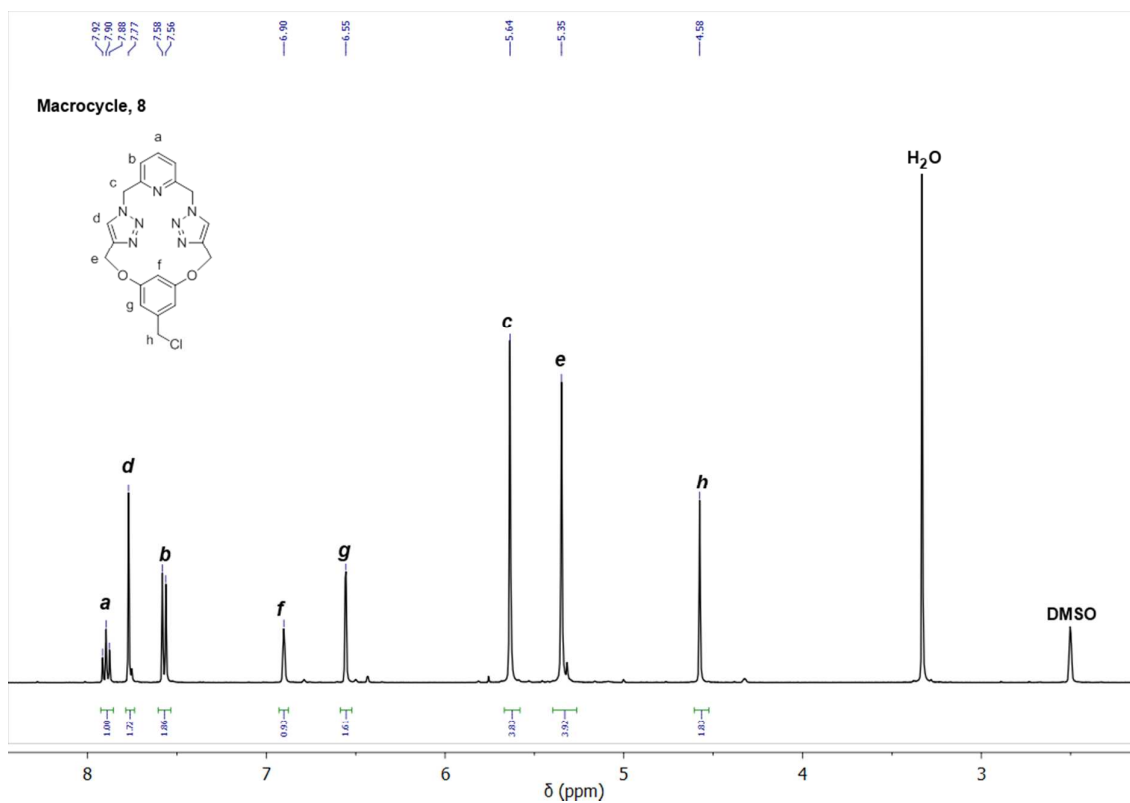
Figure S 3 ^{1}H NMR spectrum (400 MHz, DMSO-d_6, 298 K) of macrocycle **8**
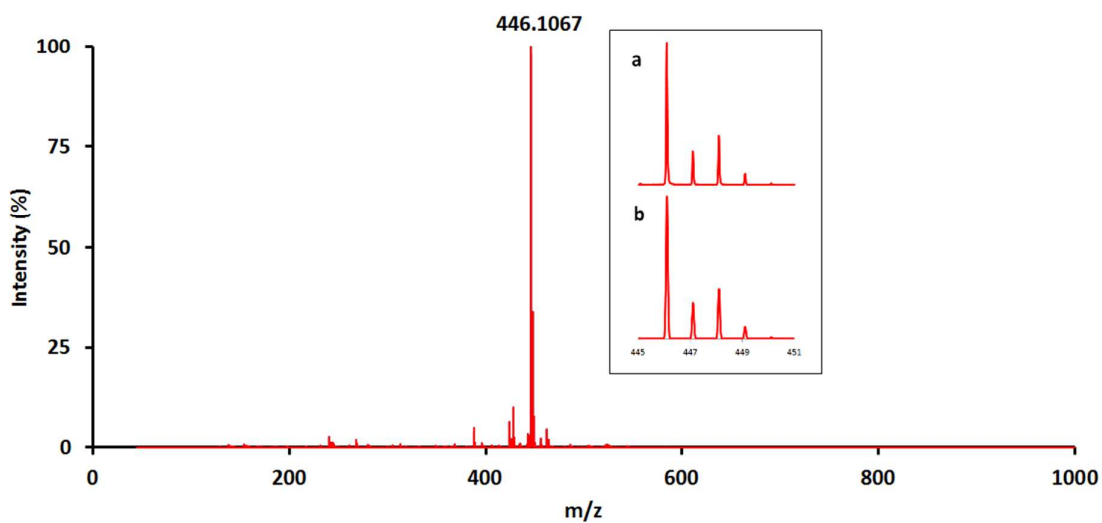
Figure S 4 HR-ESI-MS spectrum of macrocycle **8**, inset a) observed and b) calculated isotopic patterns for the peak at m/z = 446.1067 due to [**8**+Na]$^+$ ion.

Macrocycle, 9
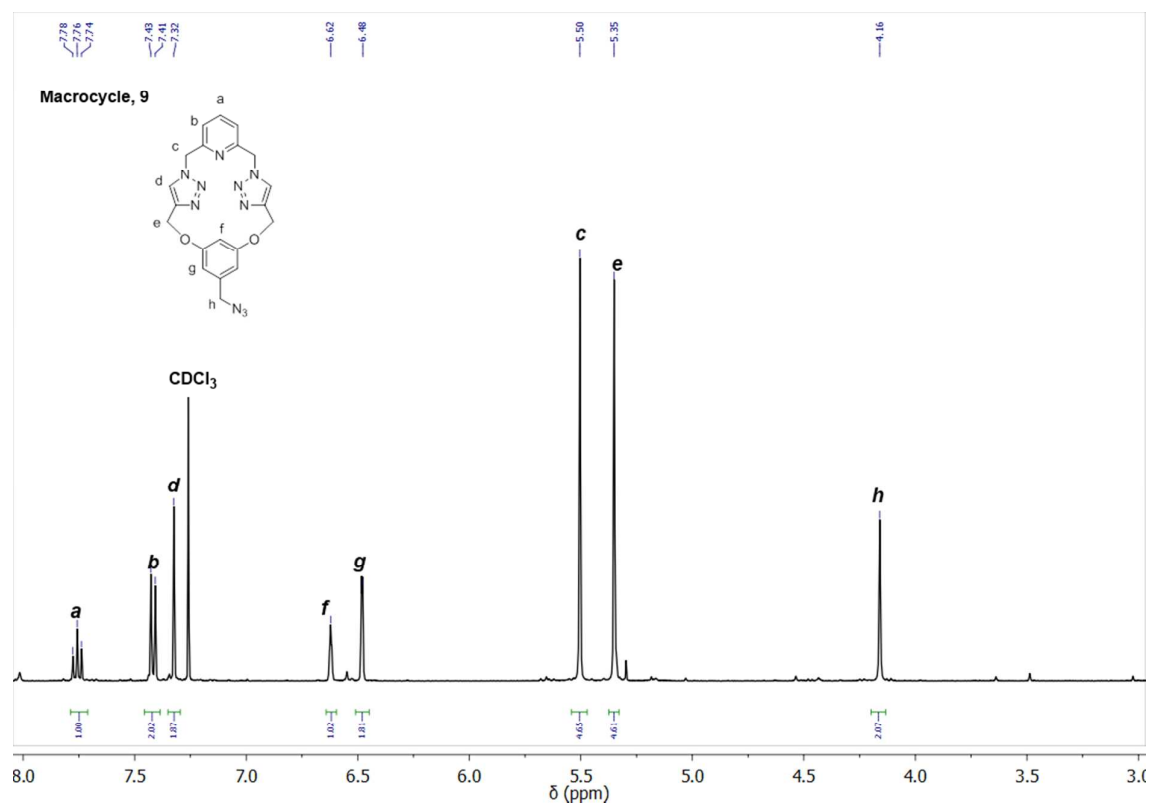
**Figure S 5** ^{1}H NMR spectrum (400 MHz, CDCl$_3$, 298 K) of macrocycle **9**
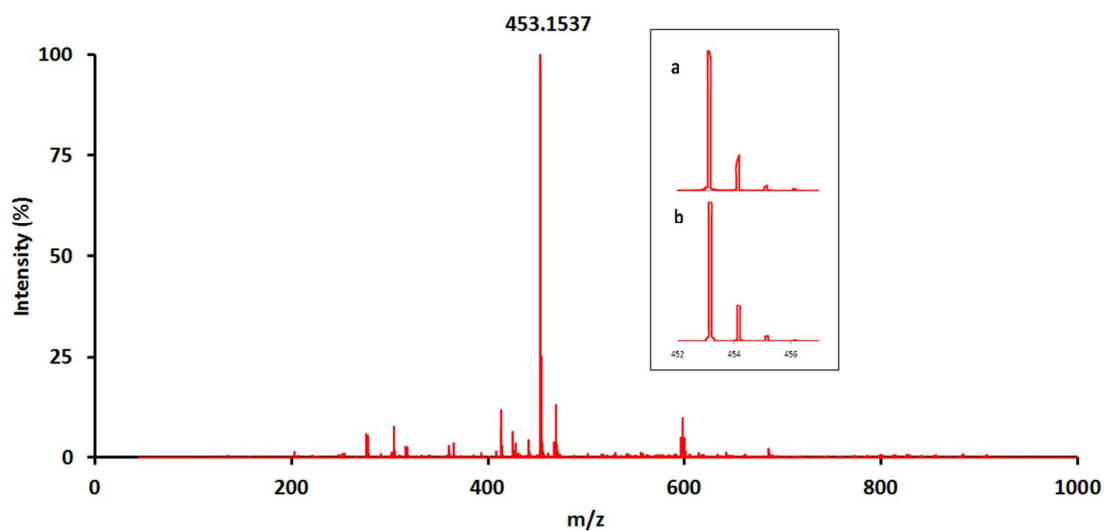
Figure S 6 HR-ESI-MS spectrum of macrocycle **9**, inset a) observed and b) calculated isotopic patterns for the peak at $m/z = 453.1537$ due to [**9**+Na]$^+$ ion.

Acid functionalized macrocycle, 10a
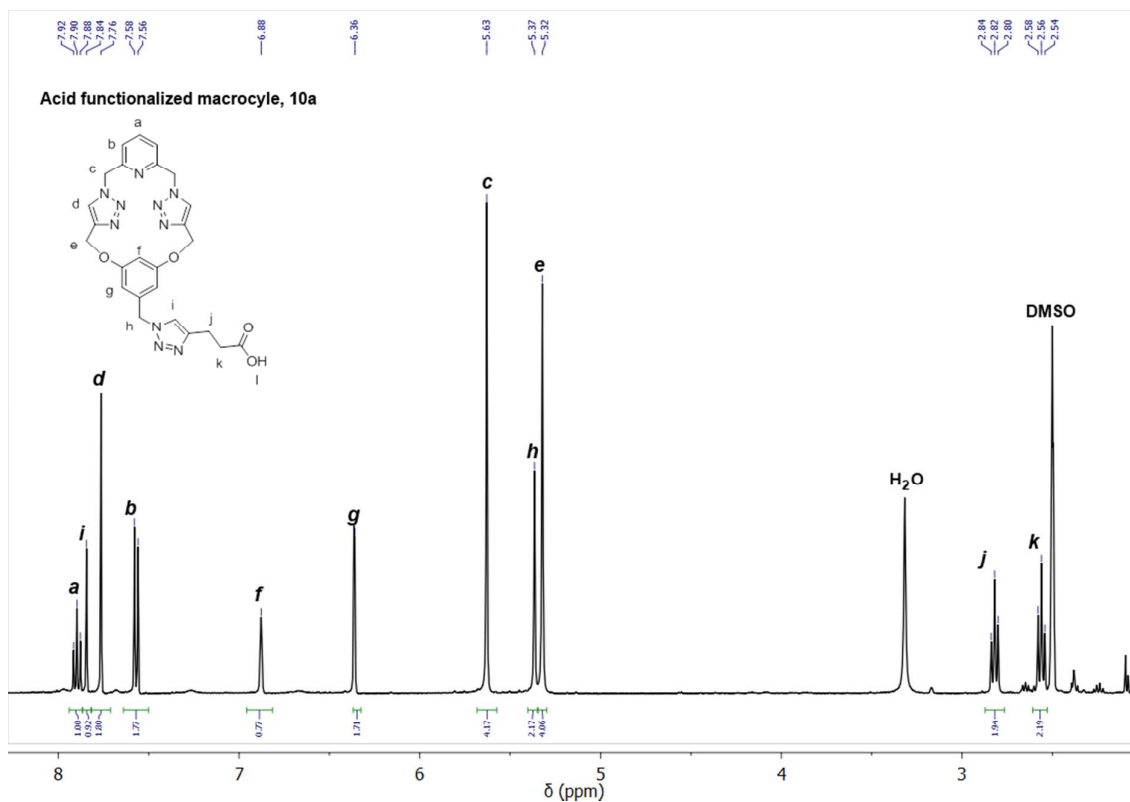
Figure S 7 ^{1}H NMR spectrum (400 MHz, DMSO-d_6, 298 K) of macrocycle **10a**
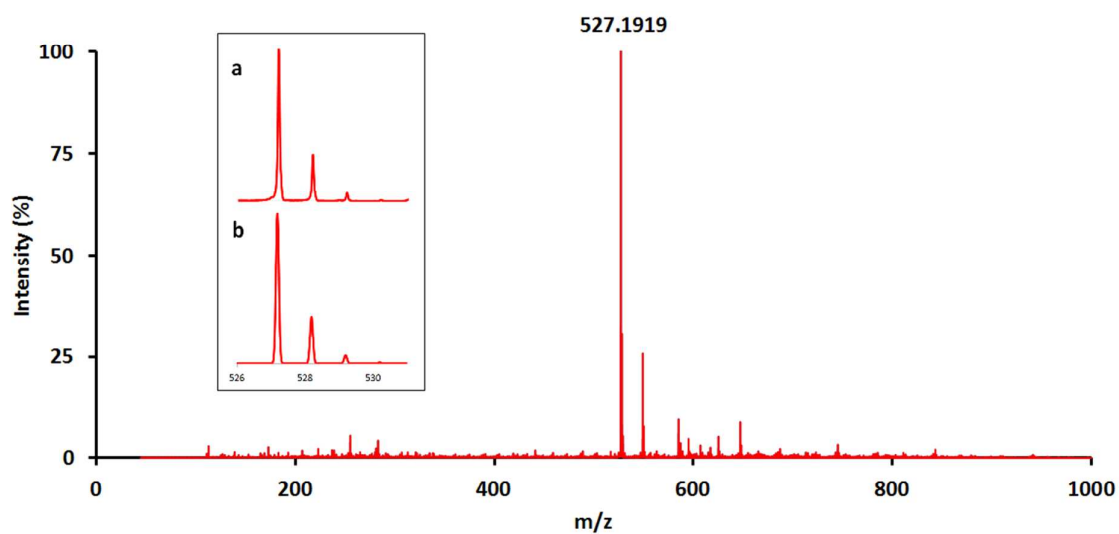
Figure S 8 HR-ESI-MS spectrum of macrocycle **10a**, inset a) observed and b) calculated isotopic patterns for the peak at m/z = 527.1919 due to [**10a**-H]$^-$ ion.

NHS activated ester functionalized macrocycle, 10b
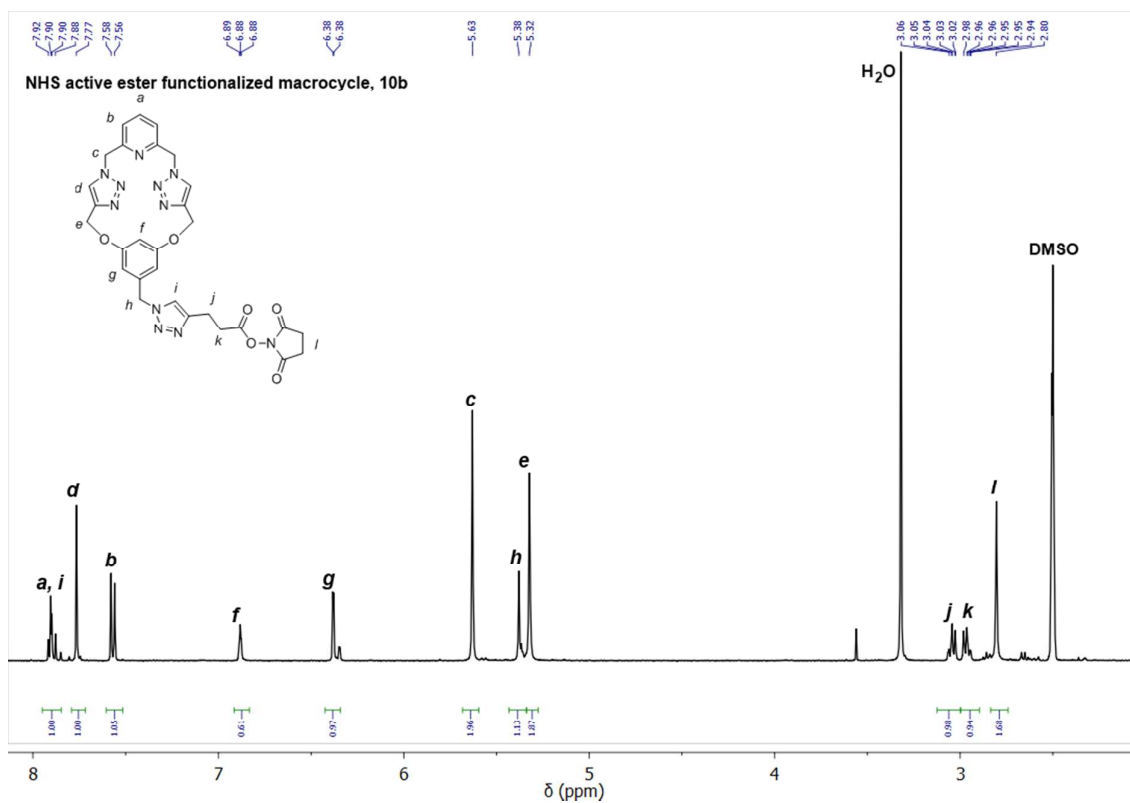
Figure S 9 ^{1}H NMR spectrum (400 MHz, DMSO-d_6, 298 K) of macrocycle **10b**.
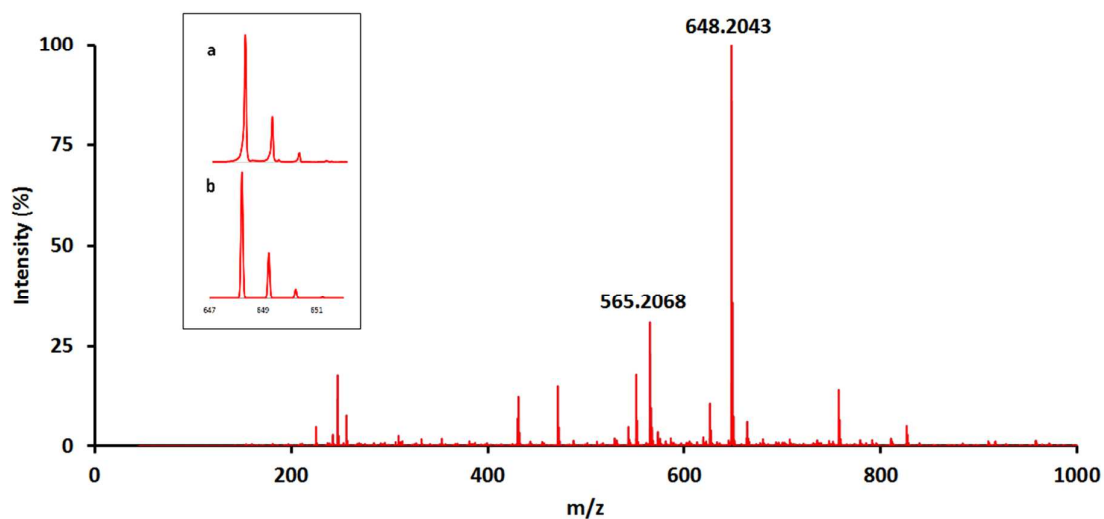

Figure S 10 HR-ESI-MS spectrum of macrocycle **10b**, inset a) observed and b) calculated isotopic patterns for the peak at m/z = 648.2043 due to [**10b**+Na]$^+$ ion, also showing peak due to [**10b**-NHS+CH$_3$+Na]$^+$ at m/z = 565.2068.

Gluco-conjugated macrocycle 10c
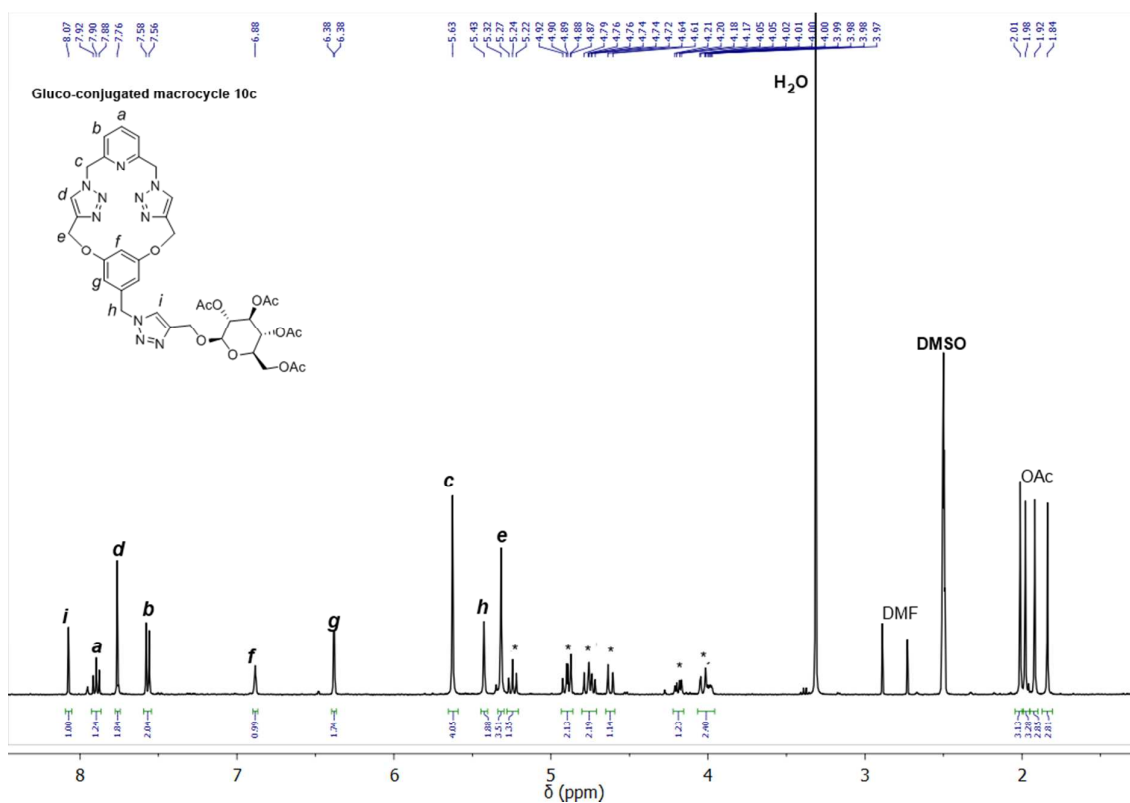
Figure S 11 ^{1}H NMR spectrum (400 MHz, DMSO-d_6, 298 K) of macrocycle **10c** (* peaks from sugar molecule).
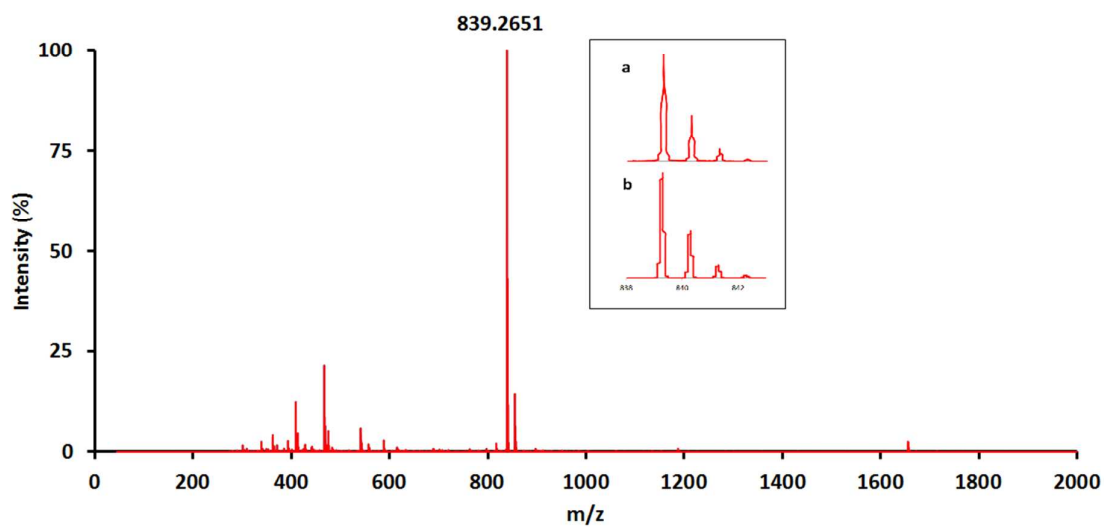

Figure S 12 HR-ESI-MS spectrum of macrocycle **10c**, inset a) observed and b) calculated isotopic patterns for the peak at m/z = 839.2651 due to [**10c**+Na]$^+$ ion.

Gluco-conjugated macrocycle 10d
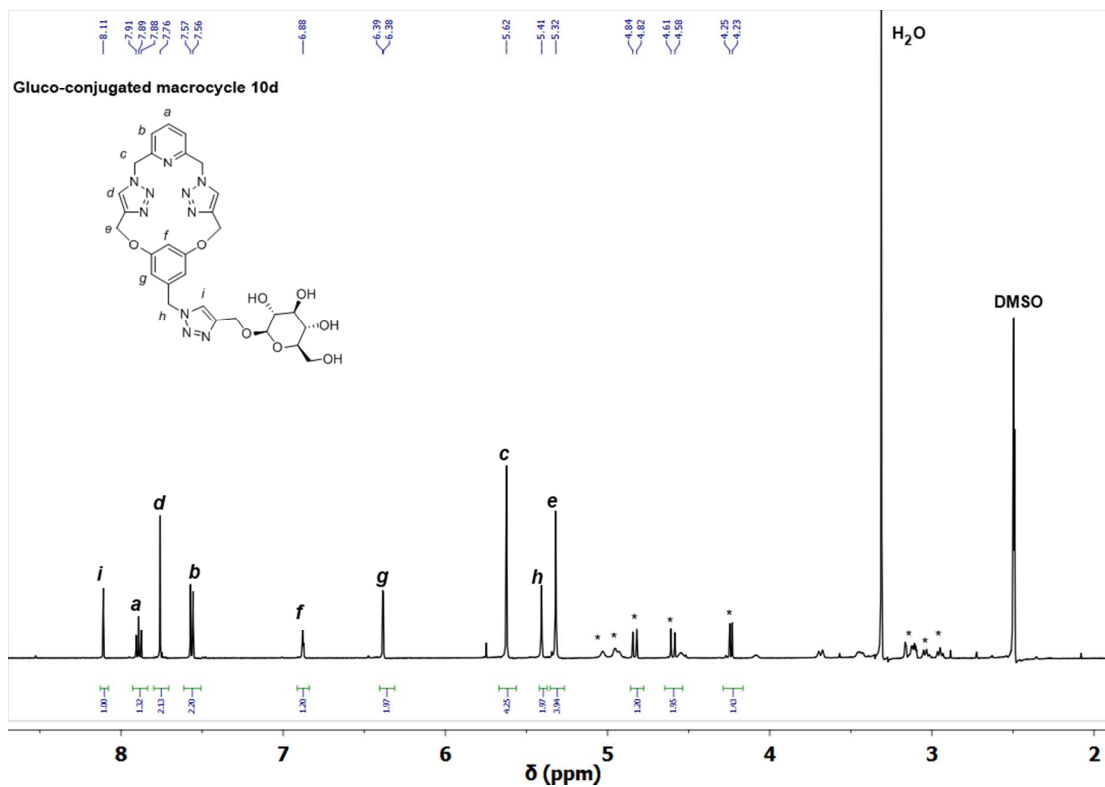
Figure S 13 ^{1}H NMR spectrum (500 MHz, DMSO-d_6, 298 K) of macrocycle **10d** (* peaks from sugar molecule).
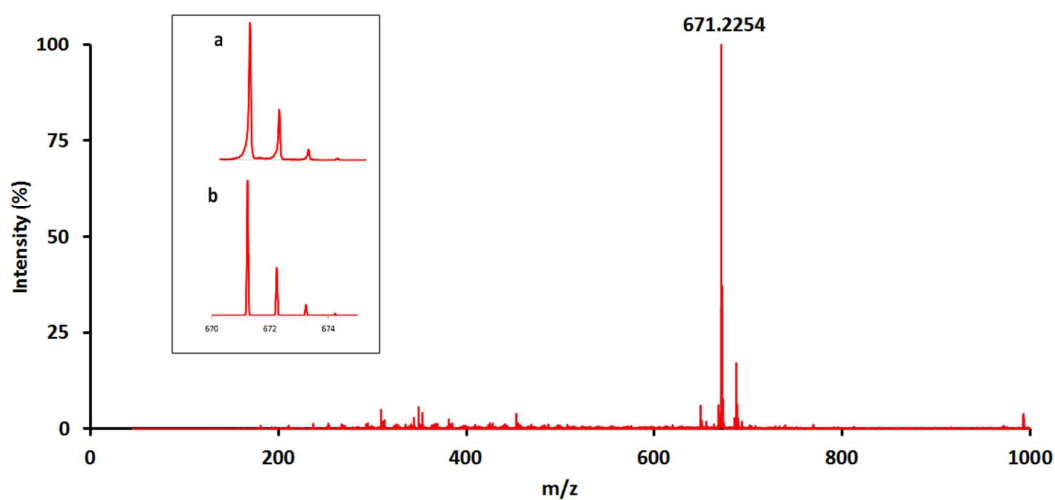
Figure S 14 HR-ESI-MS spectrum of macrocycle **10d**, inset a) observed and b) calculated isotopic patterns for the peak at m/z = 671.2254 due to [**10d**+Na]$^+$ ion.

Steroid-conjugated macrocycle 10e
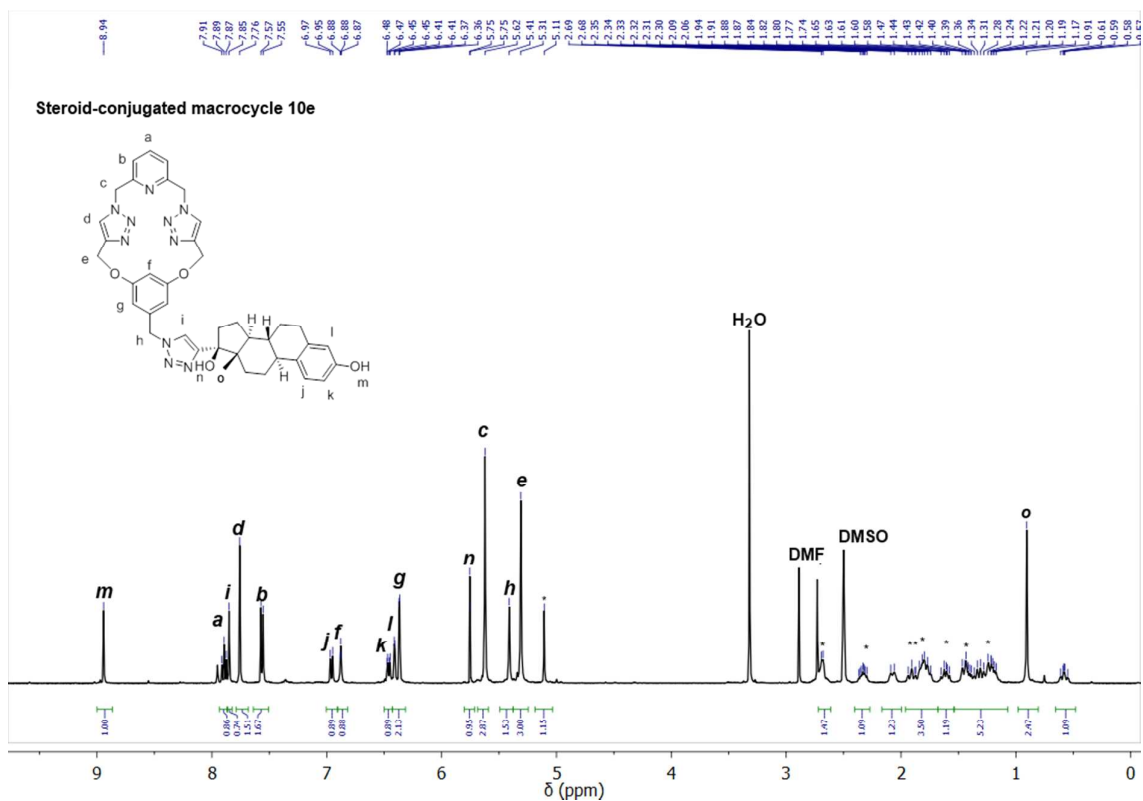
**Figure S 15** ^{1}H NMR spectrum (400 MHz, DMSO-d_6, 298 K) of macrocycle **10e** (* peaks from steroid molecule).
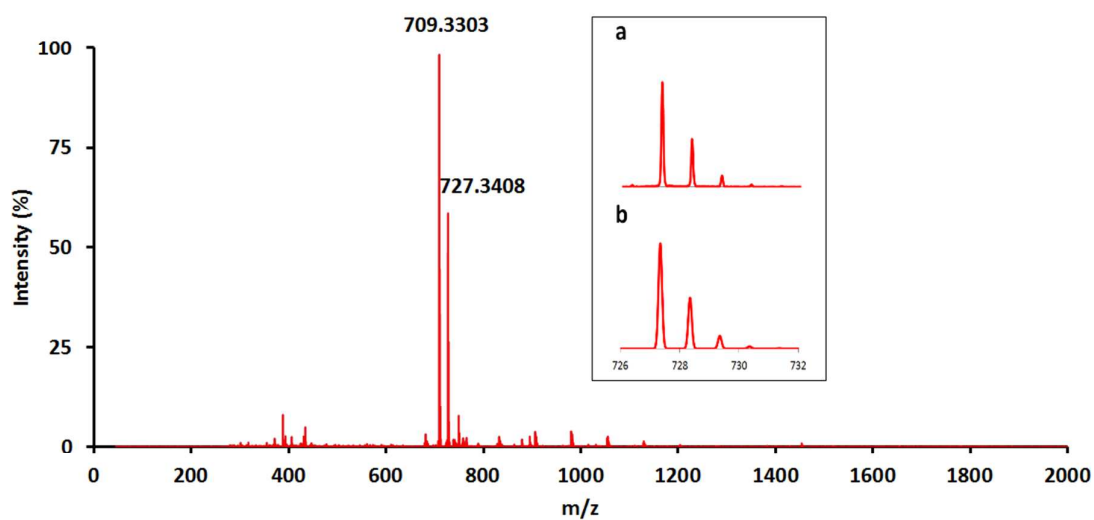
Figure S 16 HR-ESI-MS spectrum of macrocycle **10e**, inset a) observed and b) calculated isotopic patterns for the peak at m/z = 727.3408 due to [**10e**+H]$^+$ ion.

[Re(CO)₃(7)]Br, (7-Re)
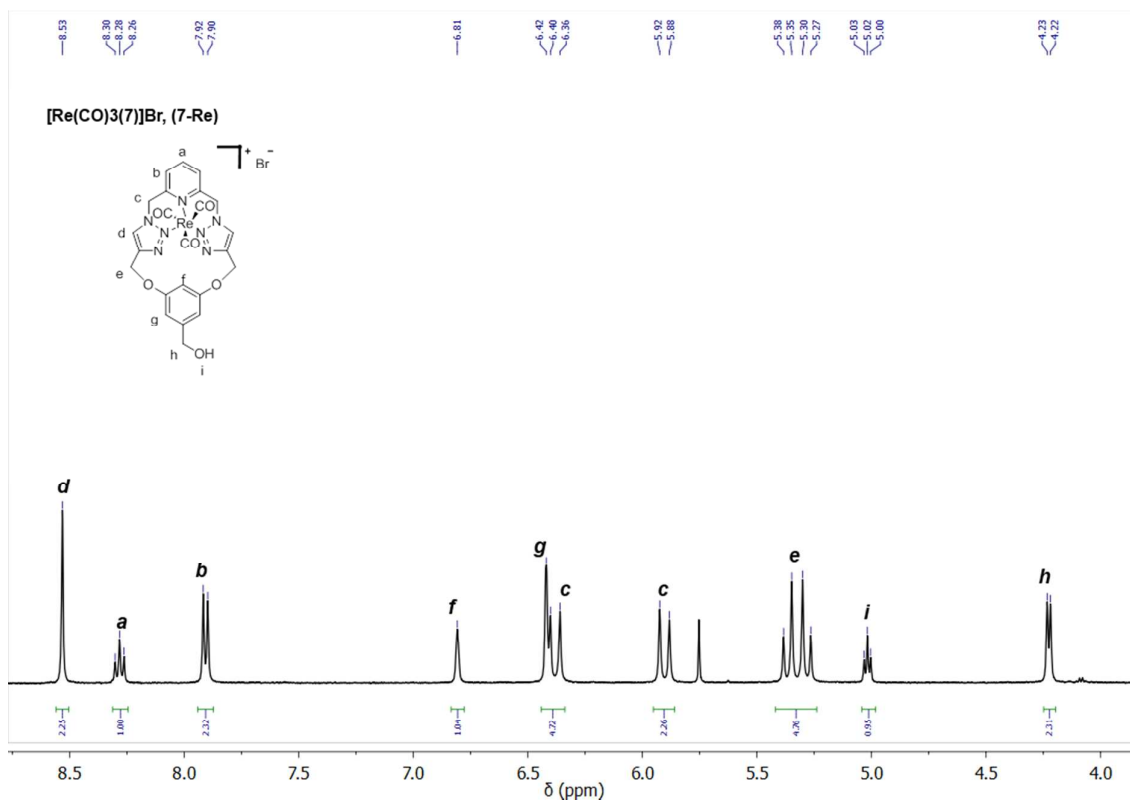
Figure S 17 ^{1}H NMR spectrum (400 MHz, DMSO-d_6, 298 K) of macrocycle **7-Re**.
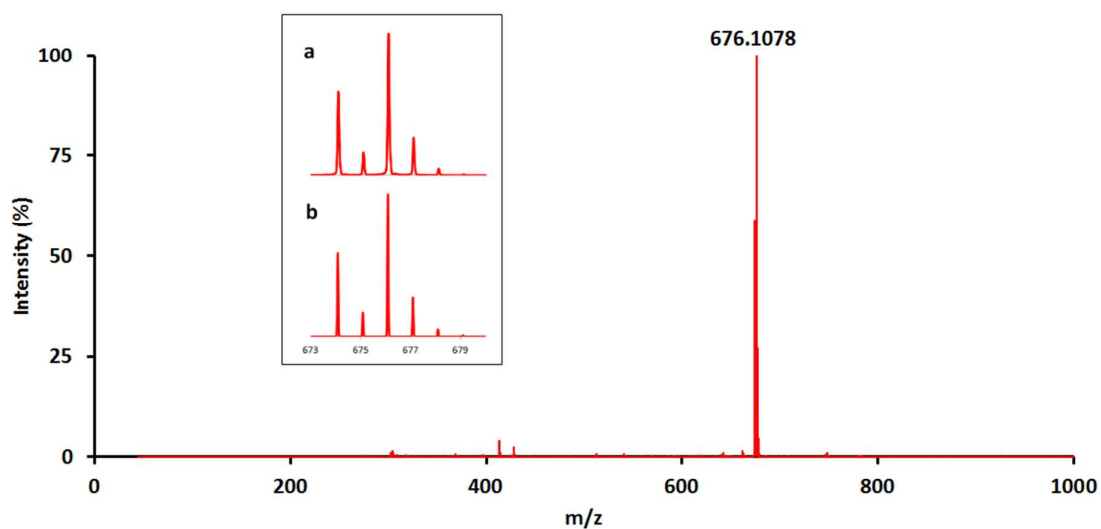

Figure S 18 HR-ESI-MS spectrum of macrocycle **7-Re**, inset a) observed and b) calculated isotopic patterns for the peak at $m/z = 676.1078$ due to [Re(CO)₃+**7**]$^{+}$ ion.

[Re(CO)₃(10a)]Br, (Re-10a)
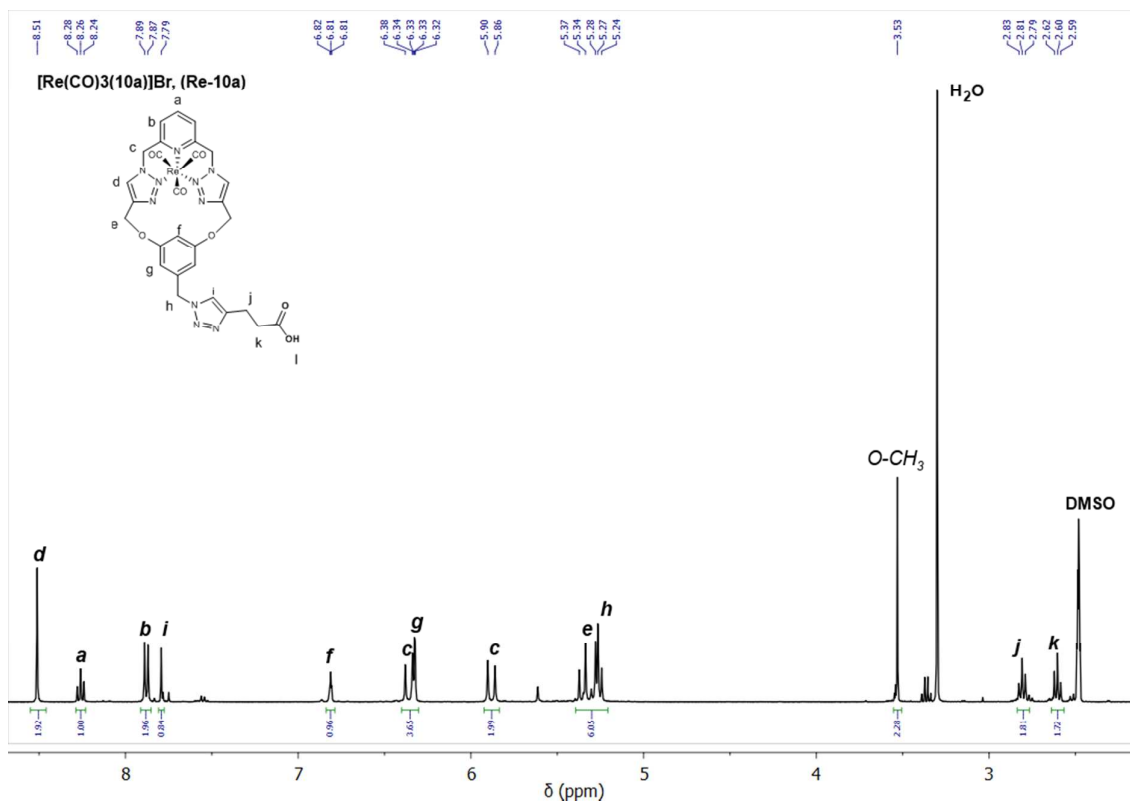
Figure S 19 ^{1}H NMR spectrum (400 MHz, DMSO-d_6, 298 K) of macrocycle **Re-10a**
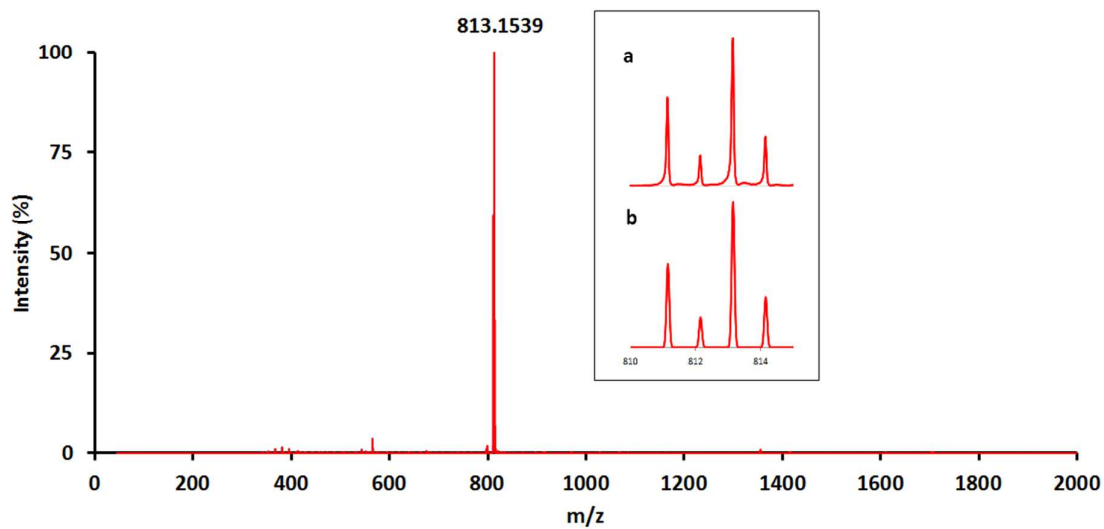
Figure S 20 HR-ESI-MS spectrum of macrocycle **Re-10a** showing peaks at m/z = 813.1539 due to esterified complex **Re-10a**, inset a) observed and b) calculated isotopic patterns for the peak at m/z = 813.1539 due to [Re(CO)₃+**10a**(-H+CH₃)]$^+$ ion.

[Re(CO)₃(10b)]Br, (Re-10b)
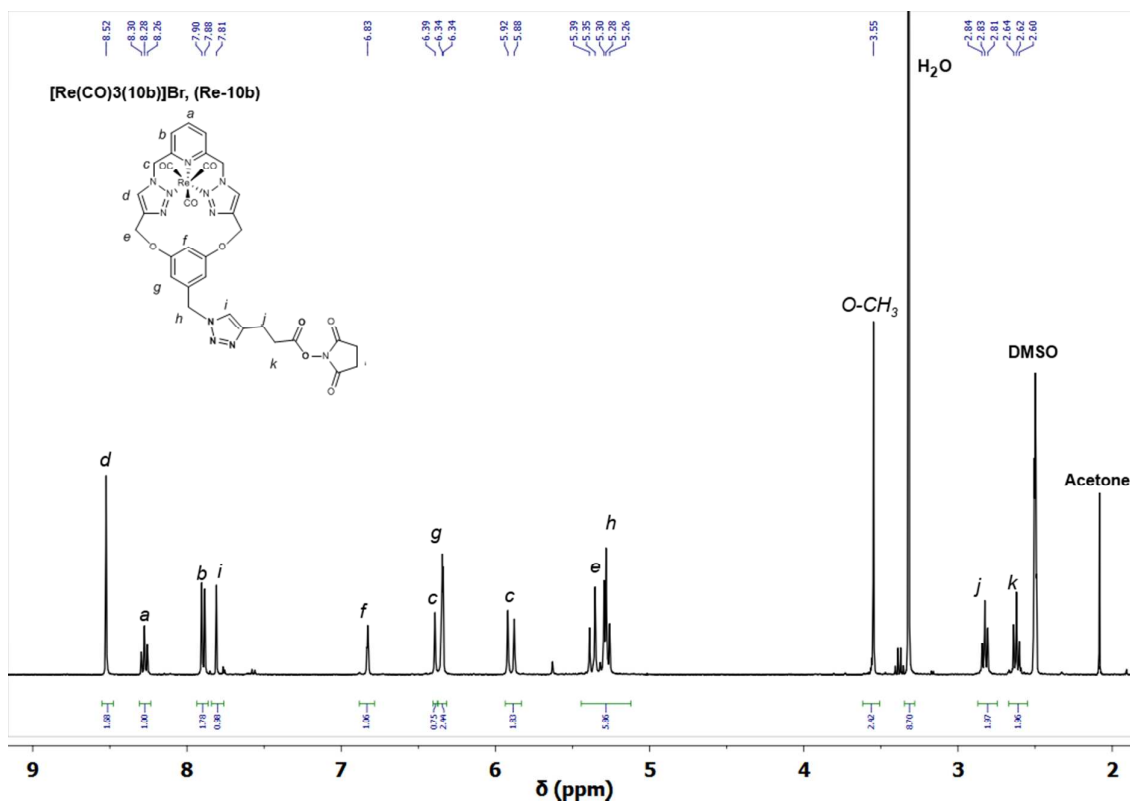
Figure S 21 ^{1}H NMR spectrum (400 MHz, DMSO-d_6, 298 K) of macrocycle **Re-10b**
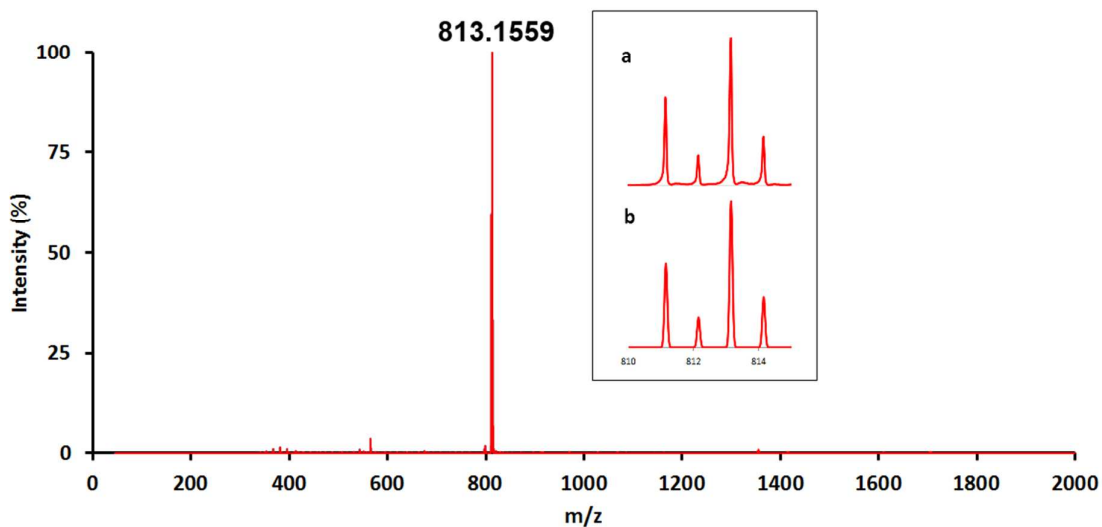
Figure S 22 HR-ESI-MS spectrum of macrocycle **Re-10b** showing peaks at m/z = 813.1559 due to esterified complex **Re-10b**, inset a) observed and b) calculated isotopic patterns for the peak at m/z = 813.1539 due to [Re(CO)₃+**10a(**-NHS+CH₃**)**]$^+$ ion.

[Re(CO)₃(10c)]Br, (Re-10c)
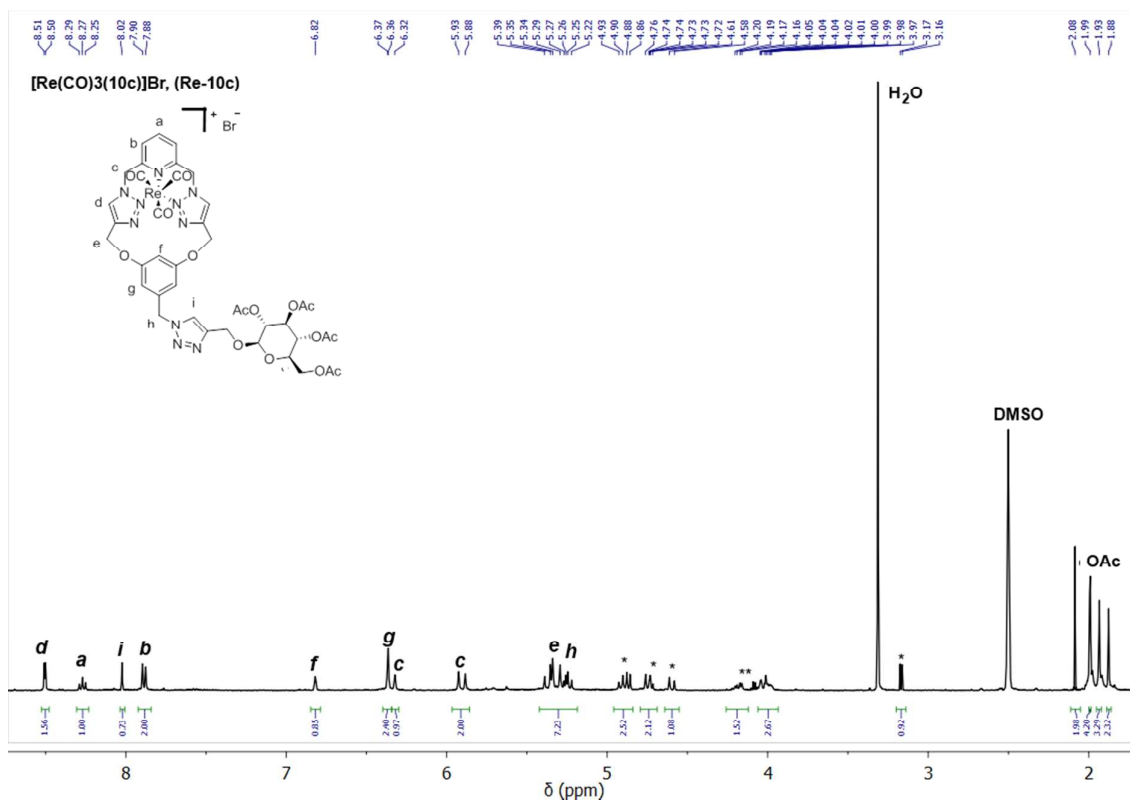
Figure S 23 ^{1}H NMR spectrum (400 MHz, DMSO-d_6, 298 K) of macrocycle **Re-10c** (* peaks from sugar molecule).
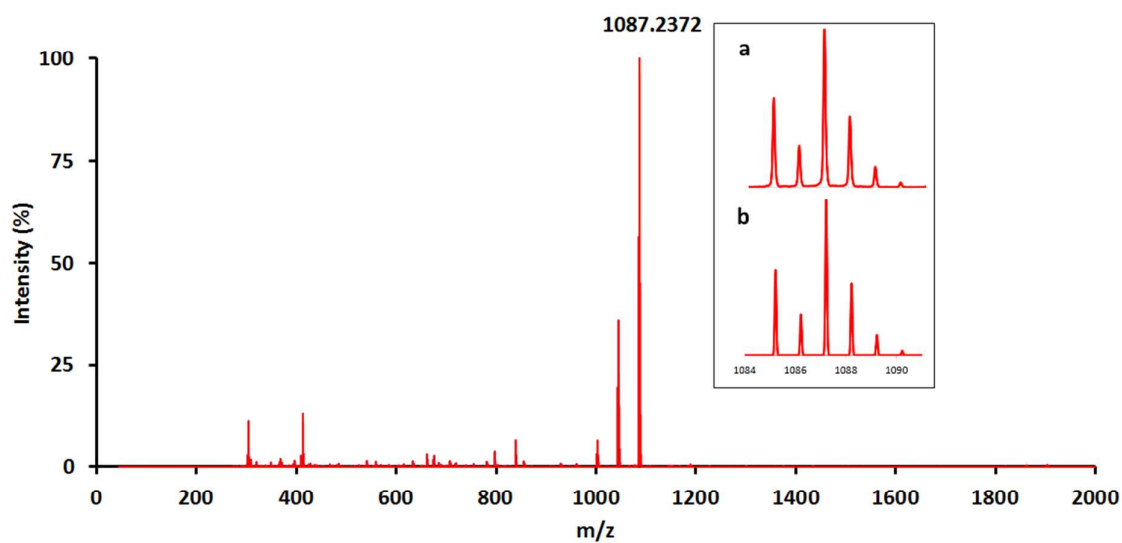

Figure S 24 HR-ESI-MS spectrum of macrocycle complex **Re-10c**, inset a) observed and b) calculated isotopic patterns for the peak at m/z = 1087.2372 due to [Re(CO)₃+**10c**]$^+$ ion.

[Re(CO)₃(10d)]Br, (Re-10d)
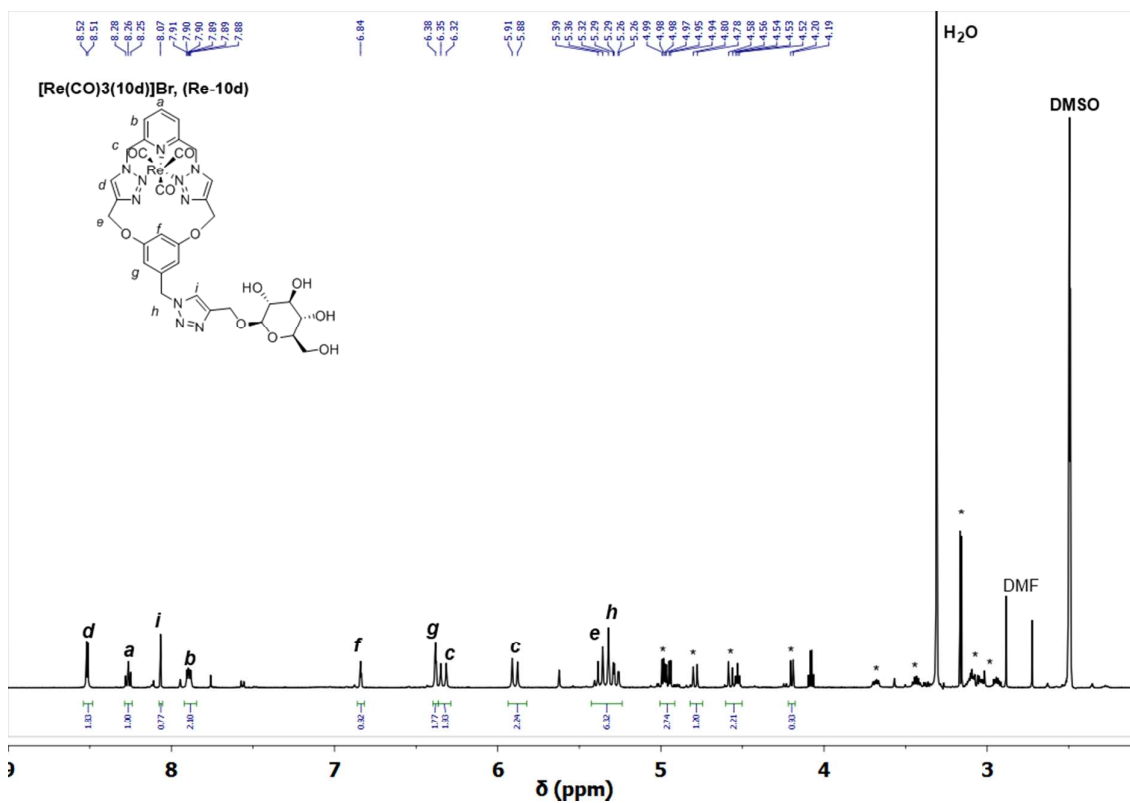
Figure S 25 ¹H NMR spectrum (500 MHz, DMSO-d_6, 298 K) of macrocycle **Re-10d** (* peaks from sugar molecule).
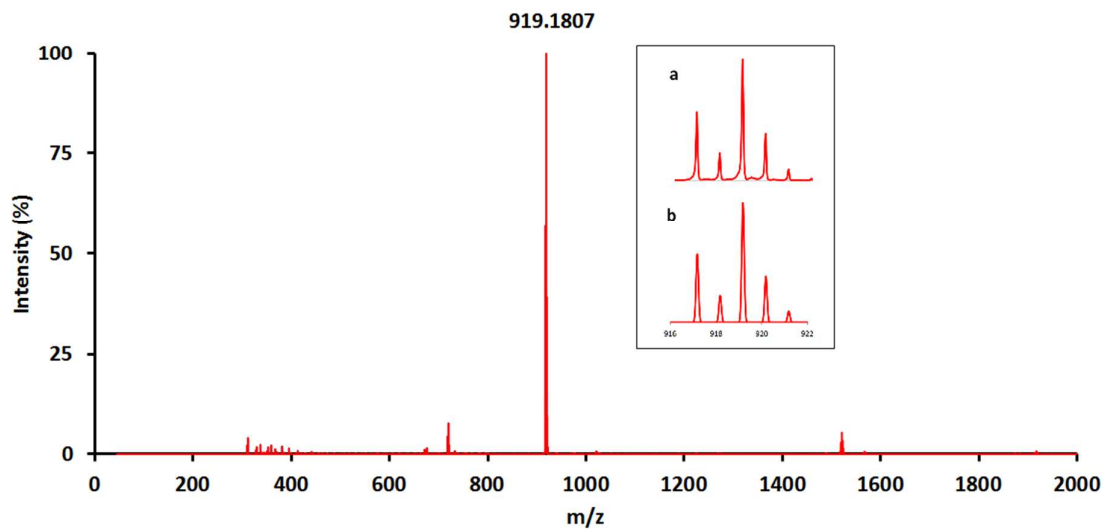

Figure S 26 HR-ESI-MS spectrum of macrocycle complex **Re-10d**, inset a) observed and b) calculated isotopic patterns for the peak at m/z = 919.1807 due to [Re(CO)₃+**10d**]⁺ ion.

[Re(CO)₃(10e)]Br, (Re-10e)
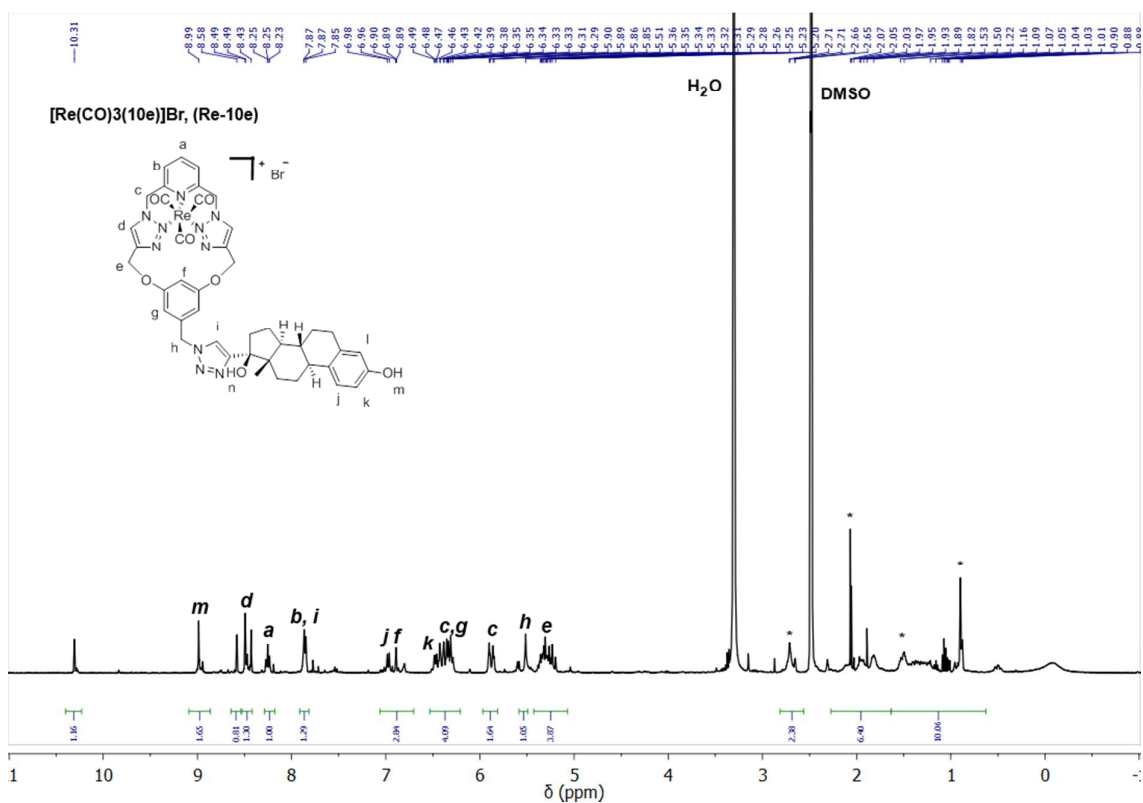
Figure S 27 ¹H NMR spectrum (400 MHz, DMSO-*d₆*, 298 K) of macrocycle **Re-10e** (* peaks from steroid molecule)
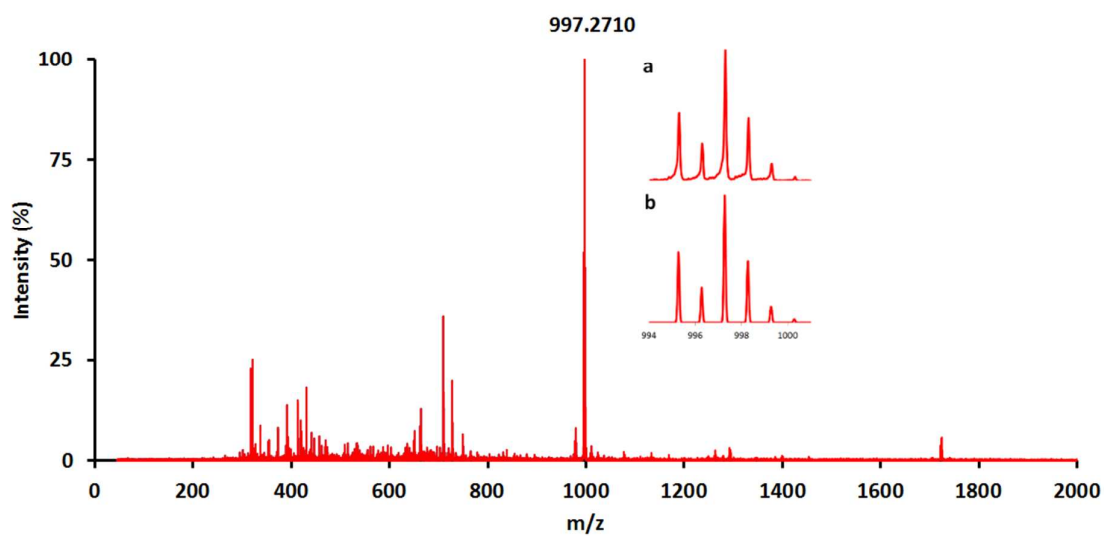
Figure S 28 HR-ESI-MS spectrum of macrocycle **Re-10e**, inset a) observed and b) calculated isotopic patterns for the peak at *m/z* = 997.2710 due to [Re(CO)₃+**10e**]⁺ ion.

[Re(CO)₃(10f)]Br, (Re-10f)
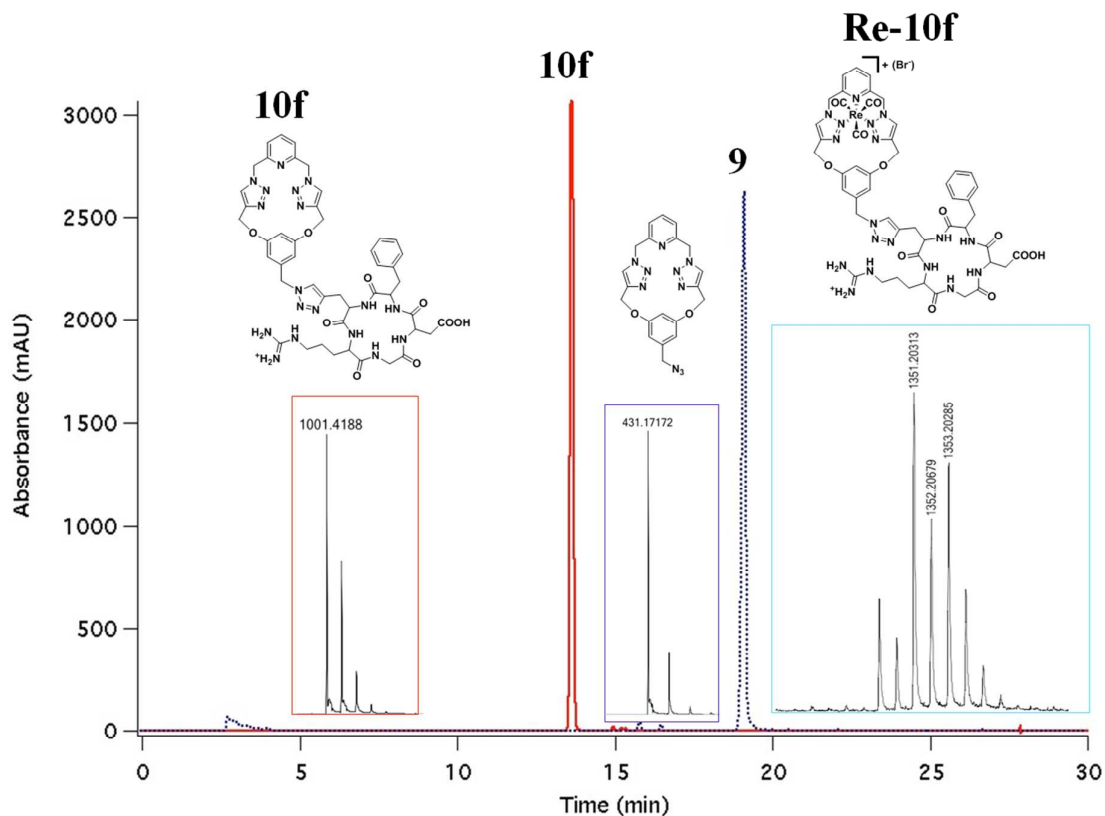
Figure S 29 RP-HPLC traces for **10f** (Method: 0-60% CH₃CN), **9** (Method: 0-100% CH₃CN) and observed ESI-MS isotopic patterns for **10f** (*m/z* = 1001.4188), **9** (*m/z* = 431.1717) and **Re-10f** (*m/z* = 1351.2031).

2 Selected stacked ¹H NMR spectra of the ligands and metal complexes
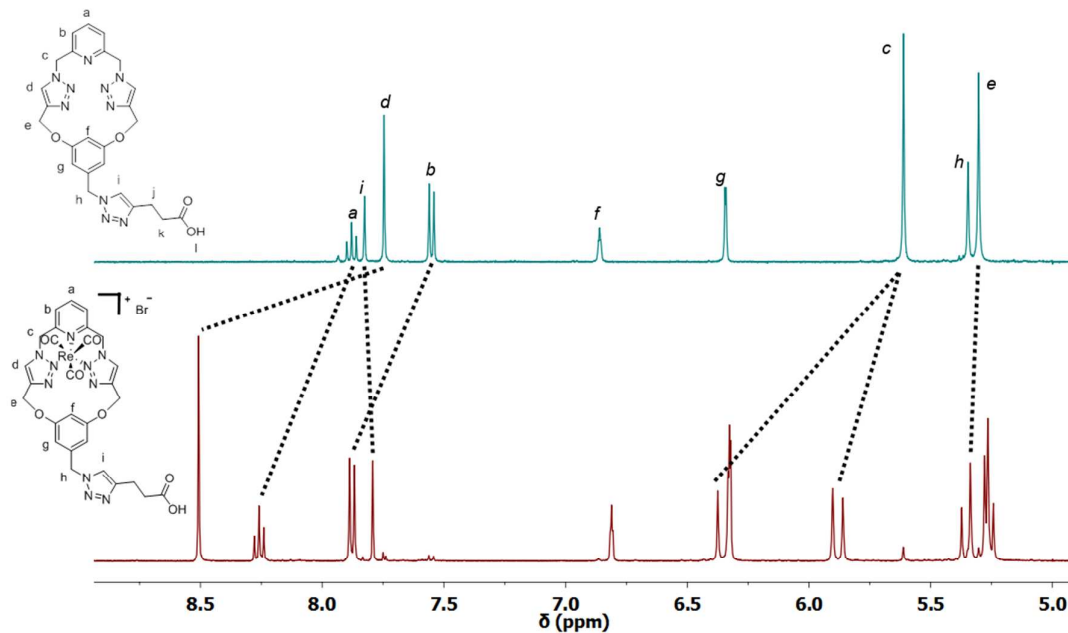
Figure S 30 Partial stacked ¹H NMR spectra (400 MHz, DMSO-d_6, 298 K) of acid-conjugated macrocycle **10a** and [Re(CO)$_3$]$^+$ complex **Re-10a**.
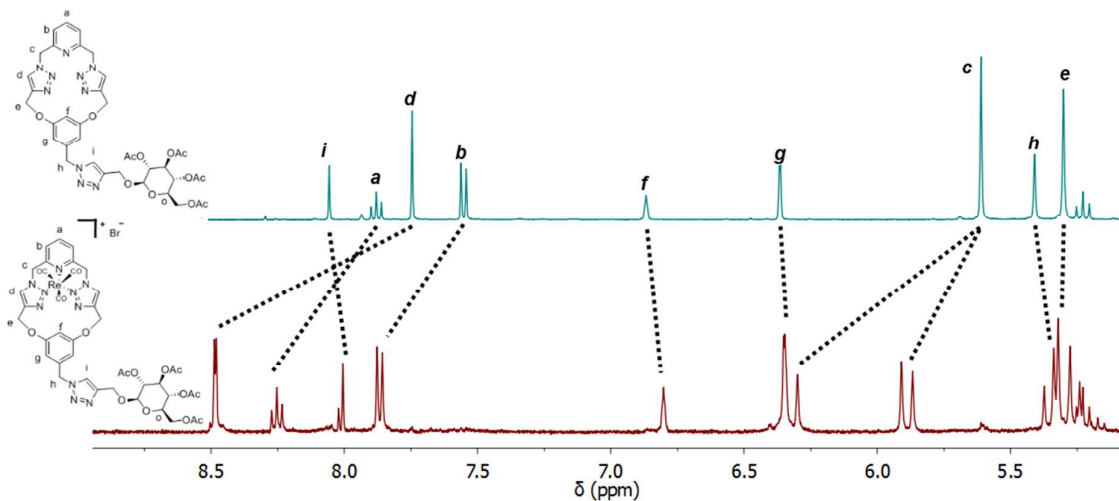
Figure S 31 Partial stacked ¹H NMR spectra (400 MHz, DMSO-d_6, 298 K) of sugar-conjugated macrocycle **10c** and [Re(CO)$_3$]$^+$ complex **Re-10c**.
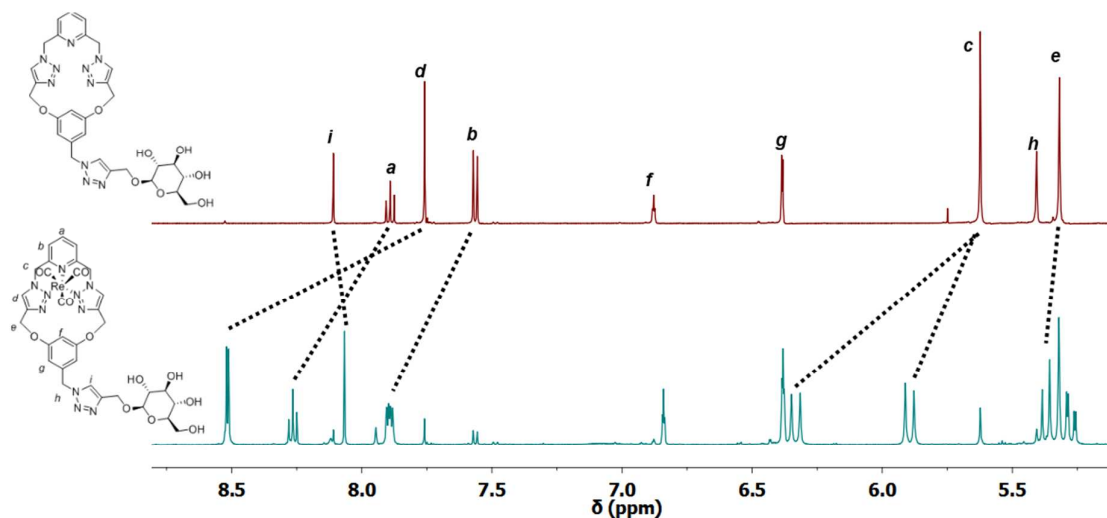
Figure S 32 Partial stacked ¹H NMR spectra (400 MHz, DMSO-d_6, 298 K) of sugar-conjugated macrocycle **10d** and $[Re(CO)_3]^+$ complex **Re-10d**.
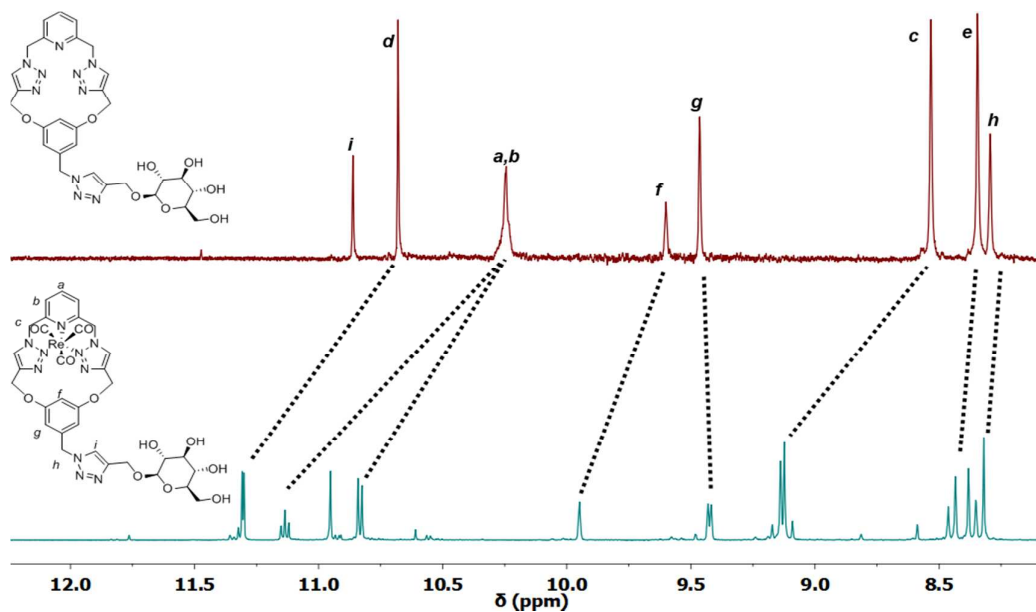
Figure S 33 Partial stacked ¹H NMR spectra (400 MHz, D₂O, 298 K) of sugar-conjugated macrocycle **10d** and $[Re(CO)_3]^+$ complex **Re-10d** showing aqueous solubility of both ligand and complex at room temperature.

3   Stability and Re(I) labelling experiments

3.1   Temperature Stability
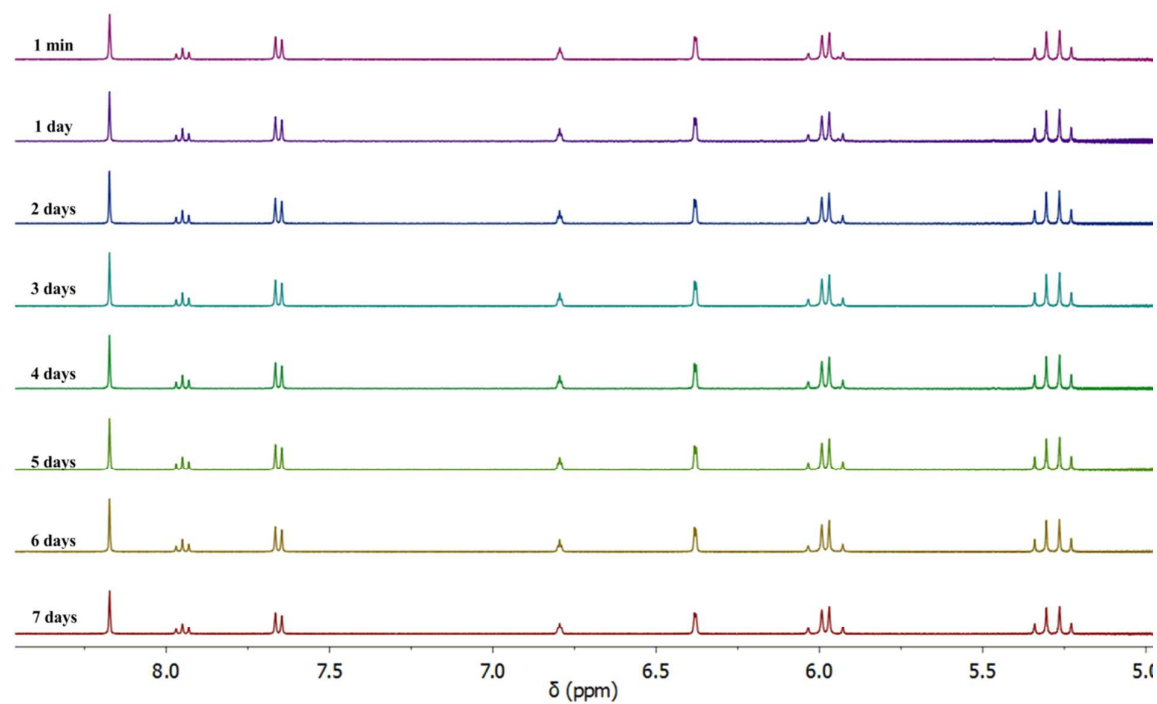
Figure S 34 Partial ^{1}H NMR spectra (400 MHz, D$_2$O, 298 K) of the Re(I) complex, **7-Re** over a period of one week**.**

3.2 Histidine competition experiments

7-Re vs Histidine
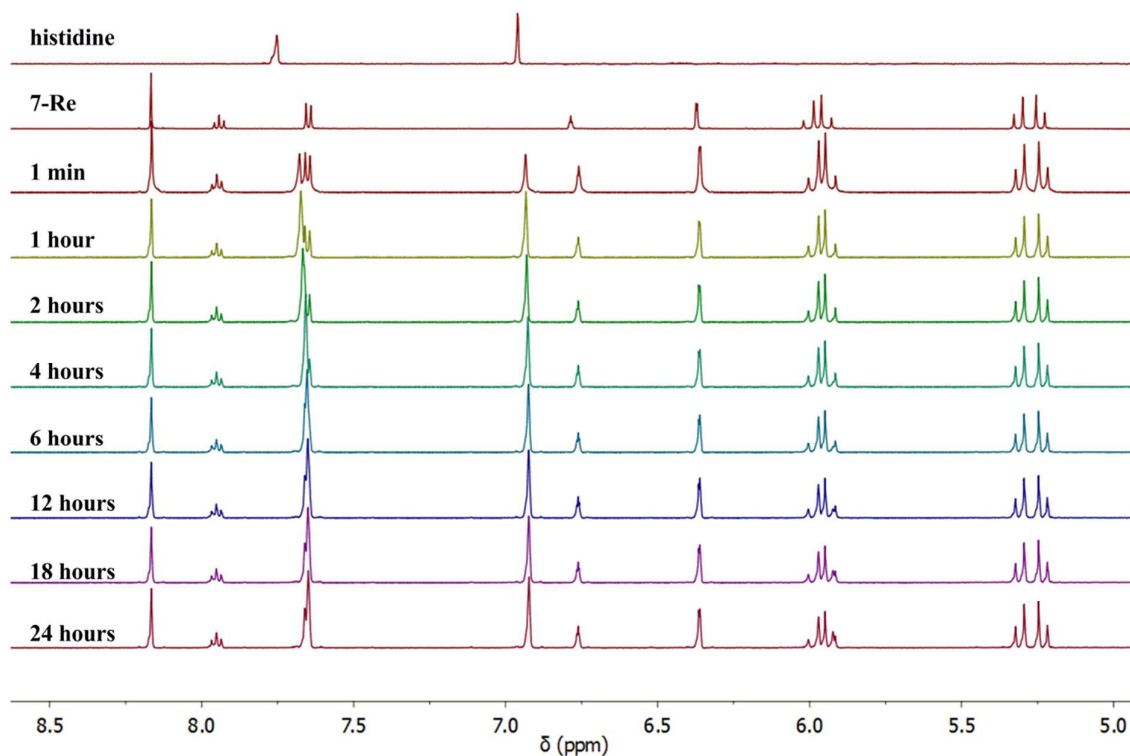
Figure S 35 Partial ^{1}H NMR spectra (500 MHz, D$_2$O, 313 K) of the histidine competition experiments showing top to bottom, histidine, the Re(I) complex **7-Re**, and the reaction mixtures of both after specified interval of time over 24 hours
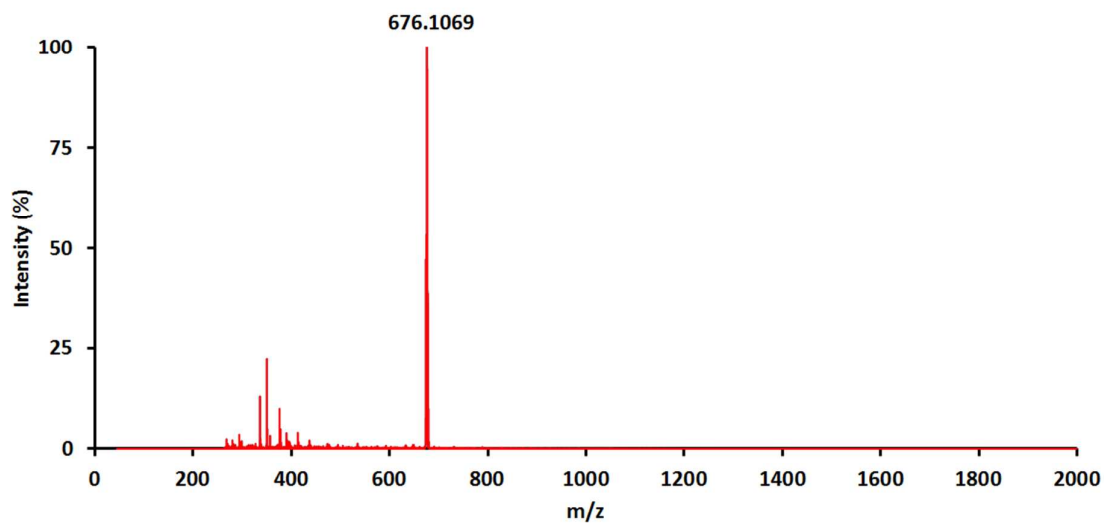
Figure S 36 HR-ESI-MS spectrum of the reaction mixture after completion of histidine competition experiment showing only major peak due to the [Re(CO)$_3$+**7**]$^+$ ions at *m/z* = 676.1069
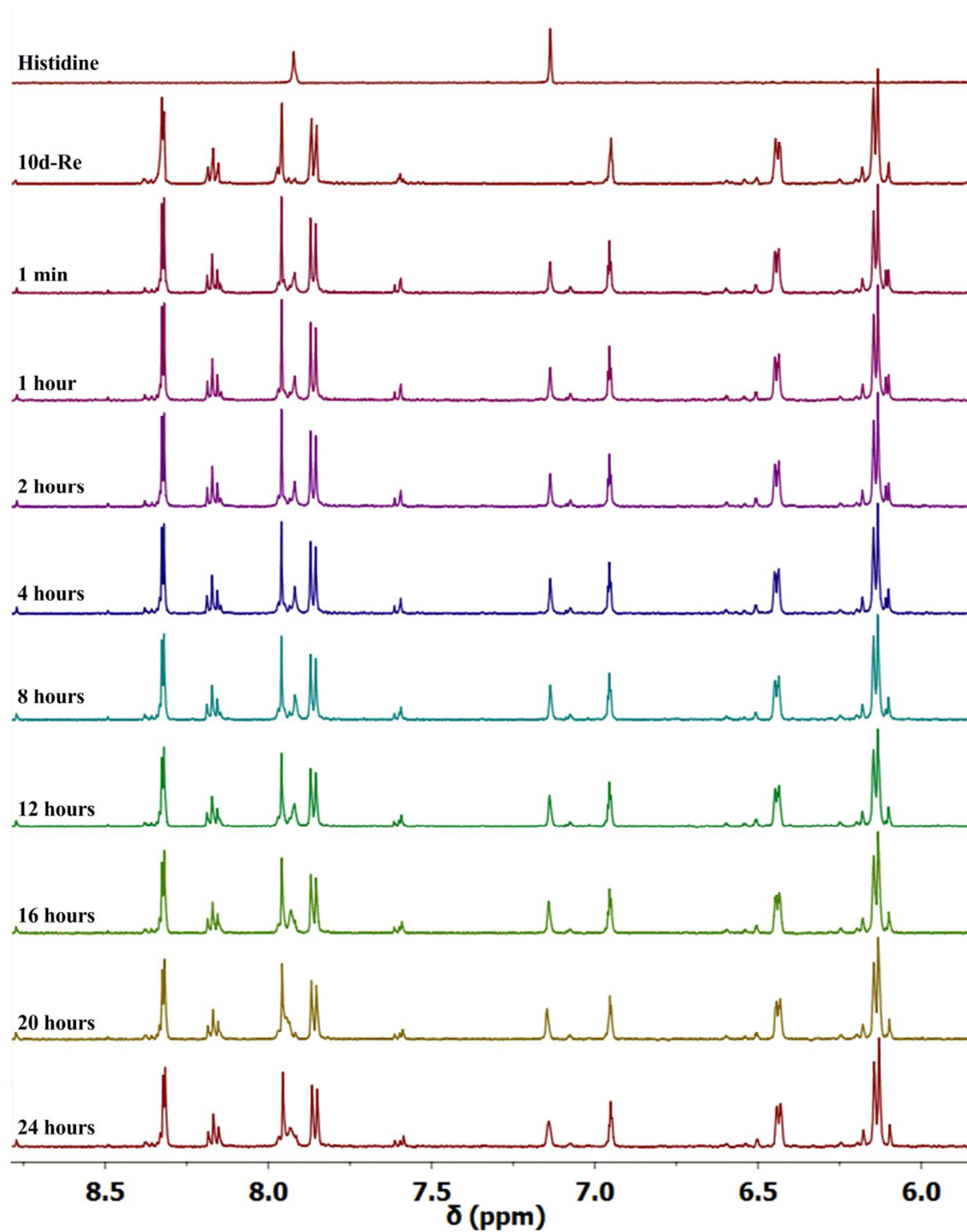
Figure S 37 Partial ^{1}H NMR spectra (500 MHz, D$_2$O, 313 K) of the histidine competition experiments showing top to bottom, histidine, the Re(I) complex **10d-Re**, and the reaction mixtures of both after specified interval of time over 24 hours
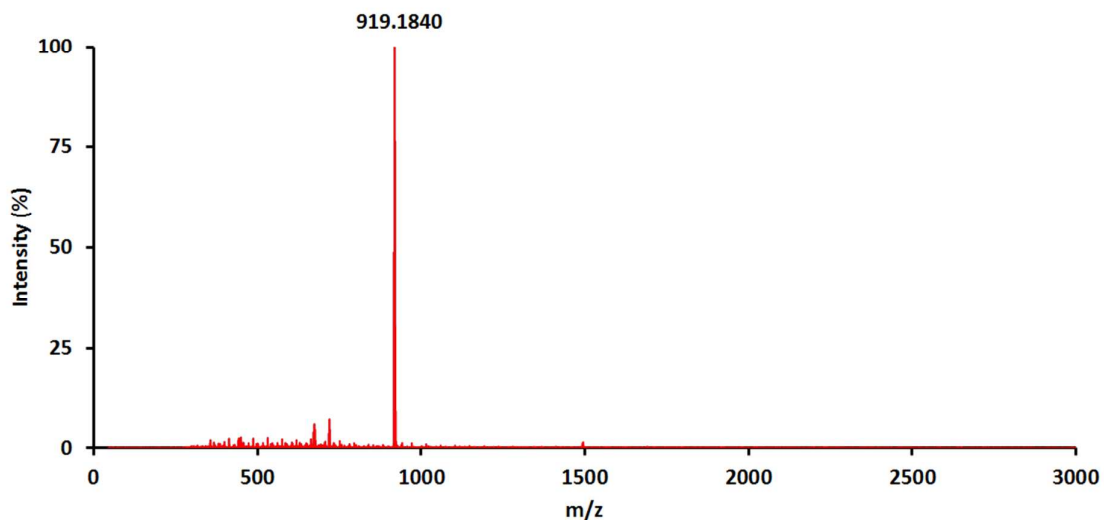
Figure S 38 HR-ESI-MS spectrum of reaction mixture after completion of histidine competition experiment showing only a major peak due to the $[Re(CO)_3+\textbf{10d}]^+$ ions at *m/z* = 919.1840

3.3 Labelling experiment of 7-Re
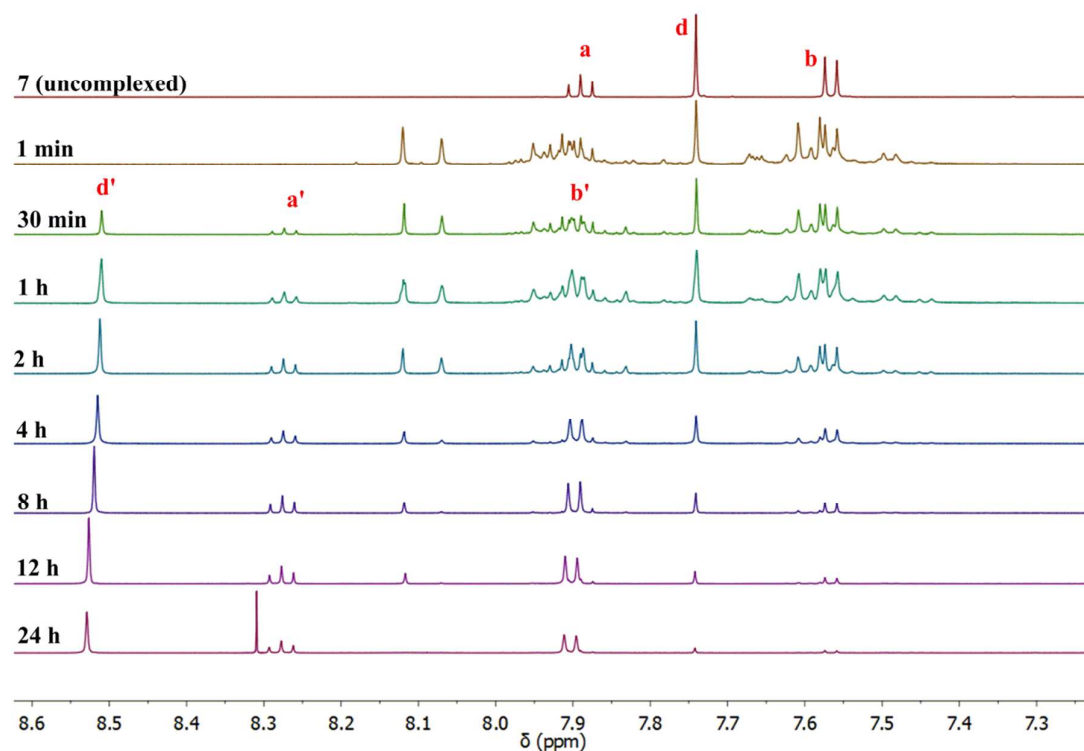
Figure S 39 Partial ^{1}H NMR spectra (500 MHz, DMSO-d_6, 298 K) of the labelling time experiments showing top to bottom, uncomplexed macrocycle **7**, and the reaction mixture containing **7** and **7-Re** after specified interval of time over 24 hours
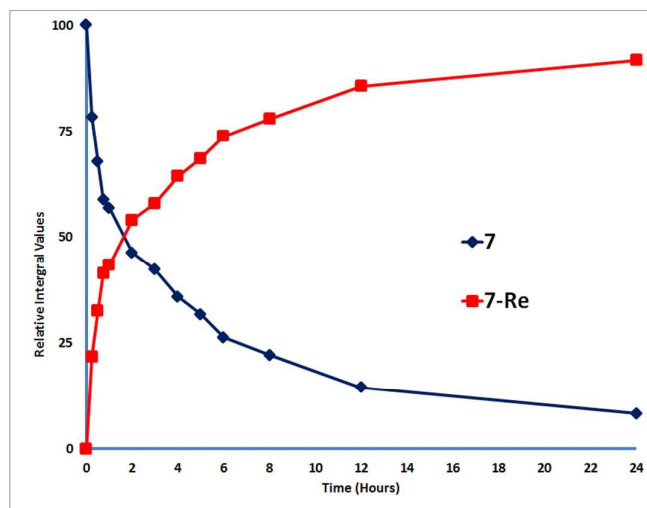
Figure S 40 Time vs integral values of the NMR labelling experiment of **7-Re**
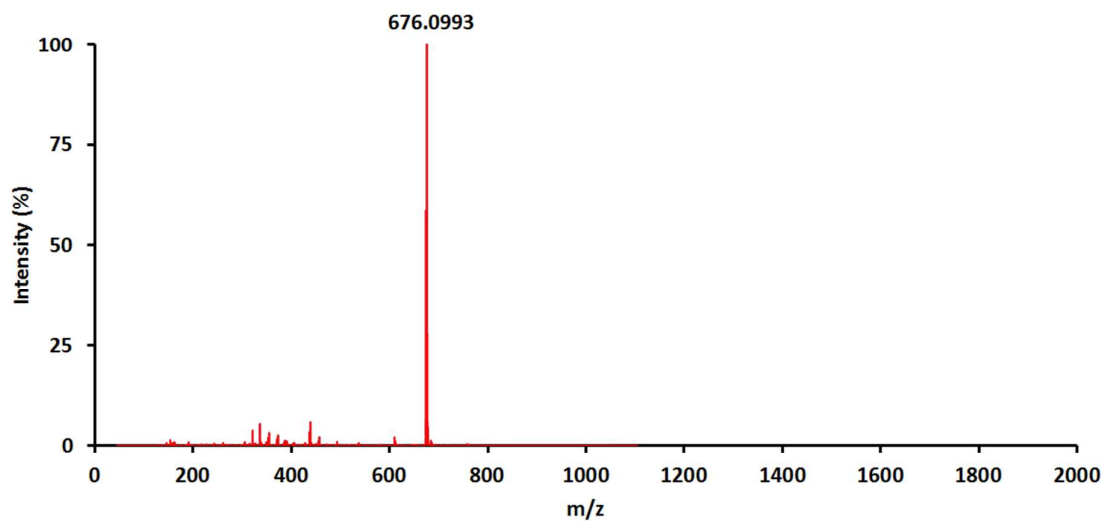
Figure S 41 HR-ESI-MS spectrum of reaction mixture after completion of labelling experiment showing only a major peak due to the $[Re(CO)_3+\mathbf{7}]^+$ ions at *m/z* 676.0993.
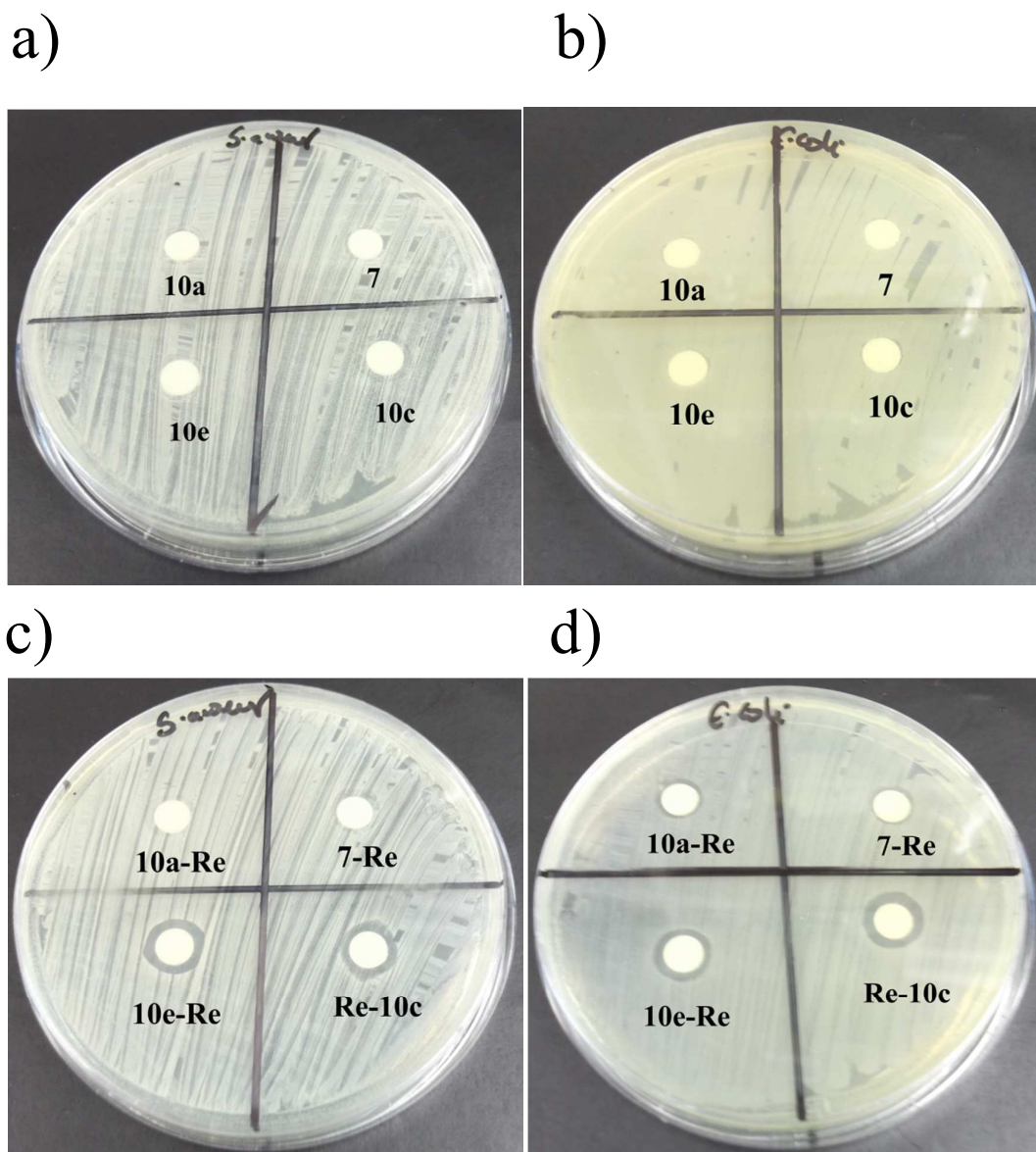
Figure S 42 a) & b) Disk diffusion assay of ligands on *S. aureus* and *E. coli*. c) & d) Disk diffusion assay of rhenium complexes on *S.aureus* and *E. coli*.

5   Photophysical Properties and Density Functional Theory Calculations

Table S 1 Calculated bond lengths and angles for **7-Re**

crystal structure		B3LYP		PBE0		CAM-B3LYP		M06		M062X	
Bond Length (Å)		Bond Length (Å)	Error	Bond Length (Å)	Error	Bond Length (Å)	Error	Bond Length (Å)	Error	Bond Length (Å)	Error
Re-N2	2.160	2.205	2.06%	2.175	0.67%	2.191	1.44%	2.200	1.86%	2.220	2.80%
Re-N4	2.252	2.306	2.41%	2.259	0.31%	2.285	1.48%	2.295	1.93%	2.324	3.19%
Re-N6	2.158	2.207	2.27%	2.177	0.87%	2.193	1.64%	2.205	2.16%	2.225	3.12%
Angle (°)		Angle (°)	Error	Angle (°)	Error	Angle (°)	Error	Angle (°)	Error	Angle (°)	Error
N4-Re-N2	79.14	79.95	1.03%	80.46	1.66%	79.98	1.06%	79.76	0.79%	78.96	0.23%
N4-Re-N6	80.44	79.90	0.68%	80.38	0.08%	79.93	0.63%	79.51	1.16%	78.69	2.18%
N2-Re-N6	86.14	89.72	4.15%	89.65	4.08%	89.45	3.84%	89.34	3.71%	89.13	3.47%
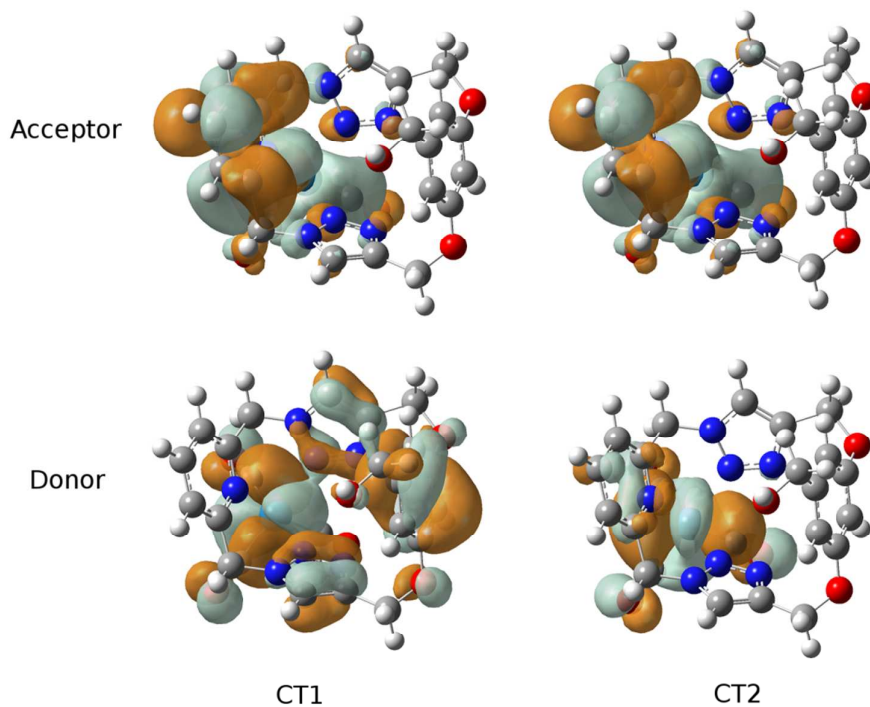
Figure S 43 Natural transitions orbitals for **7-Re** using M062X/6-31G(d)-LANL2DZ
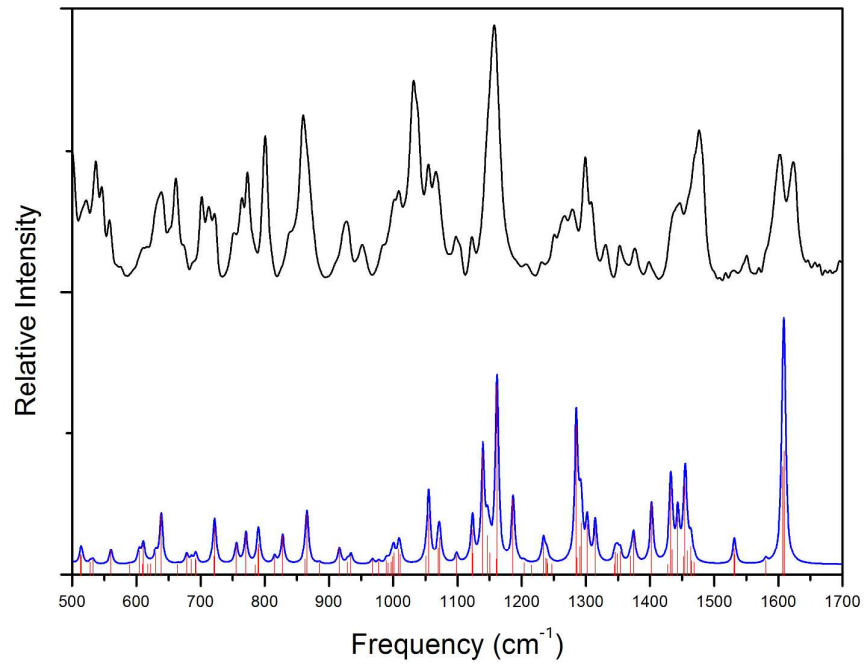
Figure S 44 ATR-IR spectrum of **7-Re** (top) and Calculated IR spectrum using CAM-B3LYP/6-31G(d)-LANL2DZ (bottom)

6 X-Ray data collection and refinement

6.1 Macrocycle (7)

X-Ray data for **7** was recorded using a Bruker APEX II CCD diffractometer using Mo-Kα radiation ($\lambda = 0.71073$ Å). The structure was solved in the monoclinic space group C2/c and refined to a R_1 value 7.2%. Hydrogen atoms were placed in calculated positions and refined using a riding model.

6.2 Re(I) complex of macrocycle (7-Re)

X-Ray data for **7-Re** was recorded using a Bruker APEX II CCD diffractometer using Mo-Kα radiation ($\lambda = 0.71073$ Å). The structure was solved in triclinic space group $P\bar{1}$ using Fourier methods and refined using SHELXL[1] to a R_1 value 6.3%. Hydrogen atoms were placed in calculated positions and refined using a riding model.

6.3 Re(I) complex of macrocycle (Re-10a)

X-ray data for macrocycle **Re-10a** was collected at 100 K on a CrysAlisPro[2], Agilent Technologies diffractometer using Mo-Kα radiation ($\lambda = 0.71073$ Å). The structure was solved by direct methods and refined against F^2 using anisotropic thermal displacement parameters for all non-hydrogen atoms using the xSeed[3] and SHELXS-97[4] program to a R_1 value 5.7%.. Hydrogen atoms were placed in calculated positions and refined using a riding model. The crystal lattice contained a small amount of diffuse electron density that could not be appropriately modelled. The SQUEEZE routine within PLATON was employed to resolve this problem. Void electron count of 58 electrons can be accounted for by four molecules of water (10 electrons each) and a molecule of methanol (18 electrons) to give a total electron count of 58.

6.4   Structure Refinement Data

Table S2 Crystal data and structure refinement for macrocycle **7**

CCDC	991260
Empirical formula	$C_{20}H_{19}N_7O_3$
Formula weight	405.42
Temperature	93(2) K
Wavelength	0.71073 Å
Crystal system	Monoclinic
Space group	C_2/c
Unit cell dimensions	a = 8.918(3) Å α = 90°.
	b = 16.352(4) Å β = 96.008(11)°.
	c = 25.482(7) Å γ = 90°.
Volume	3695.7(17) Å^3
Z	8
Density (calculated)	1.457 Mg/m^3
Absorption coefficient	0.103 mm^{-1}
F(000)	1696
Crystal size	0.22 x 0.21 x 0.05 mm^3
Theta range for data collection	1.61 to 20.21°.
Index ranges	-8<=h<=8, -15<=k<=15, -24<=l<=24
Reflections collected	11510
Independent reflections	1761 [R(int) = 0.0826]
Completeness to theta = 20.21°	99.5 %
Absorption correction	Semi-empirical from equivalents
Max. and min. transmission	0.9949 and 0.9777
Refinement method	Full-matrix least-squares on F^2
Data / restraints / parameters	1761 / 0 / 273
Goodness-of-fit on F^2	1.144
Final R indices [I>2sigma(I)]	R1 = 0.0725, wR2 = 0.1684
R indices (all data)	R1 = 0.0873, wR2 = 0.1800
Extinction coefficient	0.0024(5)
Largest diff. peak and hole	0.332 and -0.250 e.Å^{-3}

Table S3 Crystal data and structure refinement for Re(I) complex **7-Re**

CCDC	991258
Empirical formula	$C_{23}H_{19}BrN_7O_6Re$
Formula weight	755.56
Temperature	89(2) K
Wavelength	0.71073 Å
Crystal system	Triclinic
Space group	$P\bar{1}$
Unit cell dimensions	a = 9.5826(17) Å α = 66.484(11)°.
	b = 11.031(2) Å β = 76.119(11)°.
	c = 13.594(3) Å γ = 70.788(11)°.
Volume	1234.5(4) Å^3
Z	2
Density (calculated)	2.033 Mg/m^3
Absorption coefficient	6.595 mm^{-1}
F(000)	728
Crystal size	0.15 x 0.12 x 0.05 mm^3
Theta range for data collection	1.65 to 26.54°.
Index ranges	-11<=h<=11, -13<=k<=13, -17<=l<=17
Reflections collected	32686
Independent reflections	5000 [R(int) = 0.0988]
Completeness to theta = 26.54°	97.6 %
Absorption correction	Semi-empirical from equivalents
Max. and min. transmission	0.7339 and 0.4379
Refinement method	Full-matrix least-squares on F^2
Data / restraints / parameters	5000 / 0 / 344
Goodness-of-fit on F^2	1.070
Final R indices [I>2sigma(I)]	R1 = 0.0633, wR2 = 0.1573
R indices (all data)	R1 = 0.0996, wR2 = 0.1866
Largest diff. peak and hole	3.019 and -2.161 e.Å^{-3}

Table S4 Crystal data and structure refinement for **Re-10a**

CCDC	991259
Empirical formula	$C_{29}H_{26}BrN_{10}O_7Re$
Formula weight	892.71
Temperature	100.0(1) K
Wavelength	0.71073 Å
Crystal system	Triclinic
Space group	$P\bar{1}$
Unit cell dimensions	a = 10.4722(4) Å $\quad$ α = 93.303(3)°.
	b = 16.0868(8) Å $\quad$ β = 90.356(3)°.
	c = 23.1434(7) Å $\quad$ γ = 108.644(4)°.
Volume	3686.8(3) Å^3
Z	4
Density (calculated)	1.608 Mg/m^3
Absorption coefficient	4.434 mm^{-1}
F(000)	1744
Crystal size	0.20 x 0.17 x 0.06 mm^3
Theta range for data collection	2.88 to 26.37°.
Index ranges	-13<=h<=12, -20<=k<=20, -28<=l<=28
Reflections collected	31782
Independent reflections	14778 [R(int) = 0.0483]
Completeness to theta = 26.37°	98.6 %
Absorption correction	Semi-empirical from equivalents
Max. and min. transmission	0.7768 and 0.4708
Refinement method	Full-matrix least-squares on F^2
Data / restraints / parameters	14778 / 35 / 869
Goodness-of-fit on F^2	1.043
Final R indices [I>2sigma(I)]	R1 = 0.0572, wR2 = 0.1491
R indices (all data)	R1 = 0.0772, wR2 = 0.1598
Largest diff. peak and hole	2.784 and -2.246 e.Å^{-3}

Table S5 Selected bond lengths (Å) and angles (°) for **7-Re, Re-10a** and similar acyclic complex [Re(CO)$_3$(**4** R = C$_3$H$_7$)]PF$_6$ (atom labels in bold correspond to the labelling of structure **Re-10a** in **Figure S19**)

	7-Re	Re-10a	[Re(CO)$_3$(4 R = C$_3$H$_7$)]PF$_6$[5]
Bond Lenghts (Å)			
Re(1)-C(30)/**C(29)**	1.907(11)	1.906(9)	1.928(9)
Re(1)-C(32)/**C(27)**	1.917(14)	1.926(10)	1.924(5)
Re(1)-C(31)/**C(28)**	1.921(16)	1.934(10)	1.934(8)
Re(1)-N(6)	2.158(9)	2.179(6)	2.173(3)
Re(1)-N(2)/**N(3)**	2.159(9)	2.171(6)	2.155(4)
Re(1)-N(4)/**N(1)**	2.252(11)	2.241(6)	2.252(3)
Bond Angles (°)			
C(29)/C(30)-Re(1)-N(6)	92.9(5)	90.8(3)	91.47(16)
C(27)/C(32)-Re(1)-N(6)	178.4(4)	175.8(3)	176.92(15)
C(28)/C(31)-Re(1)-N(6)	91.7(4)	94.5(3)	94.64(16)
C(29)/C(30)-Re(1)-N(2)/**N(3)**	178.8(4)	177.5(3)	177.96(15)
C(27)/C(32)-Re(1)-N(2)/**N(3)**	95.5(4)	96.3(3)	95.55(16)
C(28)/C(31)-Re(1)-N(2)/**N(3)**	91.7(4)	92.5(3)	91.77(17)
N(6)-Re(1)-N(2)/**N(3)**	86.1(3)	86.9(2)	79.9(2)
C(29)/C(30)-Re(1)-N(4)/**N(1)**	101.3(5)	101.8(3)	101.35(16)
C(27)/C(32)-Re(1)-N(4)/**N(1)**	100.3(5)	98.5(3)	97.88(15)
C(28)/C(31)-Re(1)-N(4)/**N(1)**	168.2(4)	169.6(3)	169.64(15)
N(6)-Re(1)-N(4)/**N(1)**	80.3(4)	79.6(2)	80.9(2)
N(3)/N(2)-Re(1)-N(4)/**N(1)**	79.1(3)	78.7(2)	78.95(13)

7 References

1. Sheldrick, G. M., *Act. Crys. Sec. A: Found. Crys.* **2008,** *A64*, 112-122.

2. CrysAlisPro, *Agilent Technologies: Yarnton, Oxfordshire, England, 2012*.

3. Barbour, L. J., *J. Supramol. Chem.* **2001,** *1*, 189-191.

4. Sheldrick, G., *Acta Cryst.* **2008,** *A64*, 112-122.

5. Anderson, C. B.; Elliott, A. B. S.; Lewis, J. E. M.; McAdam, C. J.; Gordon, K. C.; Crowley, J. D., *Dalton Trans.* **2012,** *41*, 14625-14632.